NASA CONTRACTOR REPORT 166478

Development of A Condenser For The Dual Catalyst Water Recovery System

P. Budininkas
F. Rasouli
N. Rabadi

CONTRACT NAS2-11045
March 1983

NASA

NASA CONTRACTOR REPORT 166478

Development of A Condenser For The Dual Catalyst Water Recovery System

P. Buninkas
F. Rasouli
N. Rabadi
GATX/GARD, Inc.
Niles, Illinois 60648

Prepared for
Ames Research Center
Under Contract NAS2-11045

National Aeronautics and
Space Administration

Ames Research Center
Moffett Field, California 94035

FOREWORD

The investigation described herein was conducted by GARD, INC./ GATX during the period of August, 1981 through March, 1983 under the NASA Contract NAS2-11045. The Project Engineer was P. Dudinskas who was assisted by M. Rabadi and F. Rasouli. The Technical Monitor was P. D. Quattrone, NASA Ames Research Center, Moffett Field, California.

TABLE OF CONTENTS

LIST OF FIGURES

LIST OF TABLES

SUMMARY

The recovery of potable water from untreated urine by the catalytic method has been previously demonstrated; however, to minimize the energy requirements, the catalytic system must be integrated with an energy efficient, zero-gravity evaporative process.

The first phase of this program consisted of a study and analytical evaluation of conceptual evaporation/condensation systems suitable for integration with the catalytic water recovery method. The primary requirements for each concept were its capability to operate under zero-gravity conditions, condense recovered water from a vapor-noncondensable gas mixture, and integrate with the catalytic system. Specific energy requirements were estimated for concepts meeting the primary requirements, and the concept most suitable for integration with the catalytic system was proposed.

A three-man rate condenser capable of integration with the proposed system, condensing water vapor in presence of noncondensables and transferring the heat of condensation to feed urine was designed, fabricated, and tested. It was tested with steam/air mixtures at atmospheric and elevated pressures and integrated with an actual catalytic water recovery system. The condenser has a condensation efficiency exceeding 90% and heat transfer rate of approximately 85% of theoretical value at coolant temperatures ranging from 7°C to 80°C.

INTRODUCTION

The recovery of potable water from untreated urine vapors by the dual catalyst method has been demonstrated with both low and high vapor concentration evaporative processes. However, to minimize the energy requirements there is a need to integrate the dual catalyst system with an energy efficient, high vapor concentration, zero-gravity evaporative process.

Because the catalytic water recovery system requires oxidant gas that may comprise up to 20% of the gas/vapor stream, the presently available evaporative systems such as VCD and TIMES cannot be directly integrated with it; however, the principles of these systems may be applicable.

The objectives of this investigation were:

1. Study and analytical evaluation of evaporation/condensation concepts suitable for integration with the catalytic water recovery system,

2. Design, fabrication, and testing of a three-man condenser capable of condensing the recovered water in the presence of noncondensables with a direct heat exchange to feed urine.

To achieve the above objectives, the program consisted of the following tasks:

1. Development of System Concepts. - Several evaporation/condensation concepts were developed considering their capability to operate under zero gravity conditions, integration with the catalytic water recovery method, and condensation of recovered water in the presence of noncondensables.

2. Calculation of Energy Requirements. - Using thermodynamic and heat transfer considerations, specific energy requirements for each system

concept were calculated. The calculations were performed in the same manner for all concepts by using common basic parameters, then adding parameters specific for each system.

3. Development of a Condenser. - A three-man condenser was designed, fabricated, and tested. The condenser is suitable for integration with the system recommended on the basis of concept evaluation. Condenser operation in the presence of noncondensables was demonstrated by:

a. Tests with steam/air mixtures at atmospheric pressure,

b. Tests with steam/air mixtures at elevated pressures,

c. Tests after integration into a catalytic water recovery system.

SYSTEM CONCEPTS

Integration with Vapor Compression Distillation

One possible combination of evaporator type, latent heat return method, and condenser/separator technique is the vapor compression distillation (VCD). In this section, the integration of VCD with the dual catalyst water recovery system will be considered, and methods of heat transfer and thermodynamic calculations will be presented.

Figure 1 shows distillation with vapor compression and a rotating condenser. The vapor is withdrawn from the evaporator and mixed with the recycled vapor-gas mixture. The mixture is then heated to 250°C through a compression action before it enters the NH_3 oxidation catalyst. The hot vapor-gas mixture is then drawn into a heat exchanger where it loses its superheat before it goes into the rotating condenser where part of the vapor condenses and the rest leaves with the noncondensable gases. After tapping off a pre-calculated amount vented through the H_2O decomposition catalyst, the remaining vapor/non-condensables mixture is recycled. Oxidant gas is added to the flow at the compressor inlet. The heat transfer rate through the evaporator/condenser wall is predicted by a set of equations discussed in the following sections.

Heat Transfer Calculations at the Boiler.- The heat transfer rate per unit area in the boiler for a given flow condition (pressure, solid concentration, and still RPM) can be calculated using the equation proposed by Rohsenon:(1)

$$\frac{\dot{q}}{A} = C_{sf}\left(\frac{Cp_f \Delta T}{h_{fg}} \cdot Pr^{1.2}\right)^3 \mu_f h_{fg} \left(\frac{g(\rho_f - \rho_v)}{\sigma}\right)^{1/2}, \qquad (1)$$

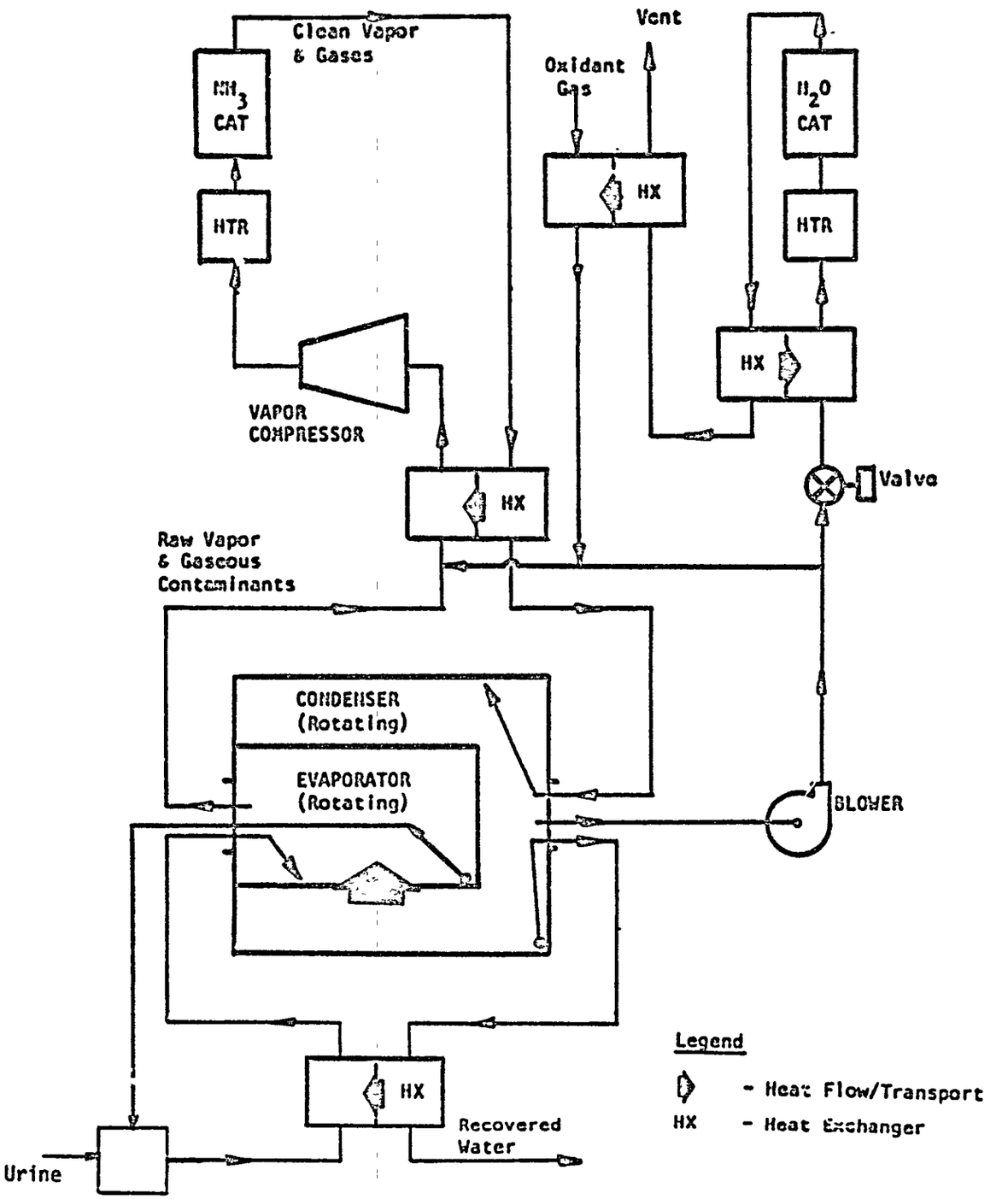

Figure 1 DUAL CATALYST SYSTEM INTEGRATED WITH VCD

where:

C_{sf} = constant which depends on the liquid and surface material

Cp = specific heat

μ = dynamic viscosity

Pr = Prandtl number

h_{fg} = heat of evaporation at boiler pressure

ρ = density

σ = surface tension

g = artificial gravity

ΔT = difference between wall and bulk temperatures

The subscripts f and v stand for liquid and vapor, respectively.

The accuracy of the results using this equation depends on the estimation of fluid properties under different flow conditions. The report written by Putnam[2] is used for calculating urine properties for solid concentrations in the urine.

Heat Transfer Calculation at the Condenser.- The rate of heat transfer on the condenser side is calculated using the analogy of a horizontal or slightly inclined plate. Rohsenon and Hartnett[3] described this process as follows: "a liquid film collects and in the quasi-steady state is continually unstable, falling off in somewhat random arrangement of drops that have approximate cosine shapes before detaching from liquid." This is usually visualized as the reverse of a film boiling on the upper side of a horizontal plate. The condensation process was analyzed and measurements were made for condensation of water at atmospheric pressure. Gertsmann and Griffith[4] correlated their results for the Nusselt number as follows.

$$Nu = 0.81\ \tau^{-0.193} \quad \text{for } \tau < 10^{-8}$$
$$Nu = 0.68\ \tau^{-0.20} \quad \text{for } 10^{-6} > \tau > 10^{-8} \qquad (2)$$

where Nu is the Nusselt number and is given by:

$$Nu = \frac{h}{K_f}\left(\frac{\sigma}{(\rho_f - \rho_v)g \cos\theta}\right) 1/2 \qquad (3)$$

and

$$\tau = \frac{K_f \mu_f \Delta T}{\rho_f (\rho_f - \rho_v)\, g \cos\theta \left(h_{fg} + \frac{3}{8} Cp_f \Delta T\right)} \left(\frac{\sigma}{g(\rho_f - \rho_v)\cos\theta}\right)^{3/2} \qquad (4)$$

where θ is the plate angle with the horizontal, h is the heat transfer coefficient at the condenser side, and K_f is the water thermal conductivity; the remaining symbols are as defined in Equation 1.

The effect of non-condensables on the rate of heat transfer at the condenser side has been quantitatively described by Sparrow and Minkowycz.[5] They show that the heat transfer rate in forced convection condensation is much less sensitive to the presence of non-condensable gases than in the case of stagnant bulk mixtures, although the reduction in heat transfer becomes more serious as the pressure is reduced. They also indicated that the reduction in heat transfer rate for both stagnant and forced convection conditions increas slightly as the difference between wall and bulk temperature increases. Figure 2 shows the effect of non-condensables on the rate of heat transfer. In the figure,which is reproduced here from Collier,[6] ϕ is the ratio between heat transfer rate with the existance of non-condensables in the stream to that which would have occurred at the same temperature difference with pure steam. These results were extrapolated for higher mass fraction of non-condensables expected to prevail in the present process.

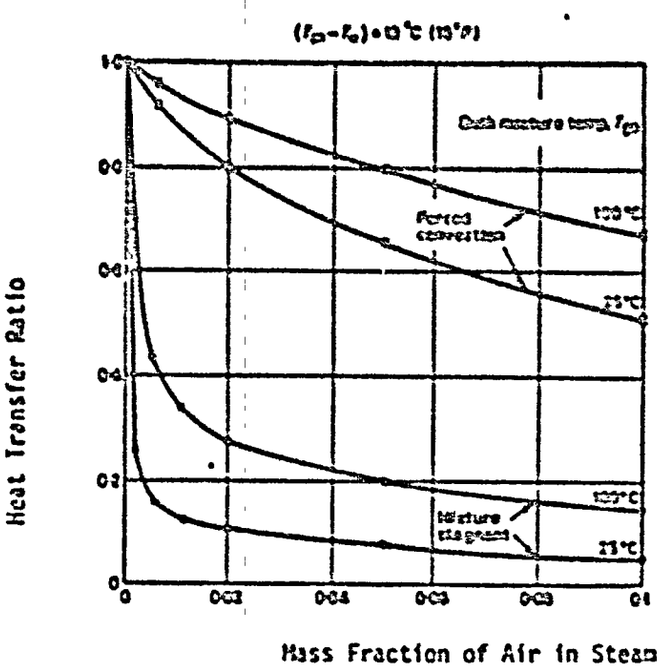

Figure 2 EFFECT OF NON-CONDENSABLES ON HEAT TRANSFER

At this point, the heat transfer rate in the condenser is calculated in two steps: 1) calculate the heat transfer assuming pure steam using equations 2 through 4, 2) use Figure 2 to include the effect of non-condensables. These calculations seem to be straight forward; however, the effect of the total pressure of the vapor-gas mixture can be as important as the air mass fraction. Sparrow et. al.[5] indicated that the reductions in steam condensation rate become more marked as the total pressure is reduced. The effect of the total pressure in the condenser is of vital importance to the present process since it determines the amount of vapor-gas mixture to be recycled.

The rate of condensation can be enhanced by several methods which can be categorized into three categories:

1) Use of force fields (centrifugal, vibrational and electrostatic) to reduce the thickness of condensate film which constitutes the major resistance.

2) Promotion of dropwise condensation through surface treatment using chemical coatings, polymer coatings, and electroplating.

3) Changes of surface geometry to increase the available area or to promote rapid removal of condensate.

All of these methods can be used to improve the rate of condensation in a VCD system condenser. The use of centrifugal force field has originally been suggested for the boiling side of the still; however, the combination of the centrifugal force field and surface geometry change can enhance the condensation rate at the condenser side of the still. This can be achieved by placing wires

along the still surface and thus generating surface tension forces to cause the condensate to flow towards the wires and to drain as rivulets alongside the wire.

Process Thermodynamics.- A thermodynamic analysis of the overall vapor compression process integrated with a dual catalytic water recovery system was conducted to provide an analytical model that is capable of correlating the effects of the basic system operating parameters. These operating parameters include boiler temperature and pressure, compressor pressure ratio, condenser temperature and pressure, mass fraction of non-condensables, and input waste solid concentration. The objective here is to calculate, for a three-man waste production rate, the heat transfer area needed for specific operating parameters with minimum specific energy, volume, and weight requirements. A computer program was written and used to calculate the design variables for different alterations of the process operation.

Figure 3 qualitatively shows the condensation/evaporation process in the presence of non-condensable gases. Liquid waste enters the boiler at point 1 and saturated steam leaves at point 2 The flow leaving the boiler is mixed with the recycled vapor-gas mixture and the oxidant gas, and the resultant mixture is then superheated by compression action to the temperature required by the NH_3 oxidation catalyst ($250^{o}C$) and pressure P_3. The mixture superheat is then removed under constant pressure bringing the vapor to point 4 at which state the mixture enters the condenser. Incomplete condensation occurs at the

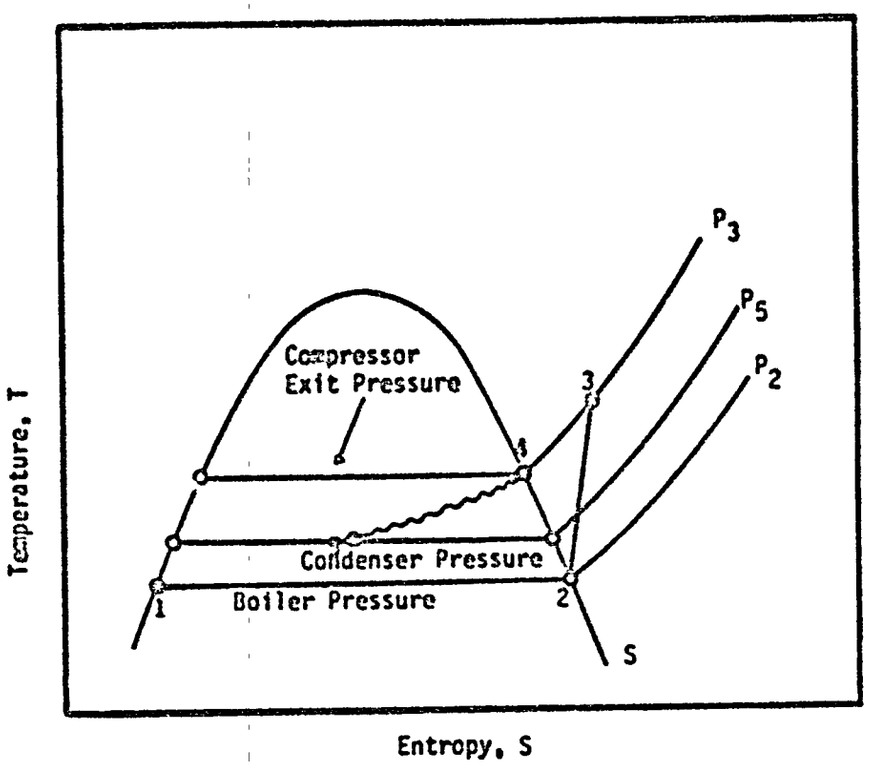

Figure 3 REPRESENTATION OF CONDENSATION IN THE PRESENCE OF NON-CONDENSABLES

condenser which brings the vapor-liquid mixture to state 5. The determination of state 5 (pressure, temperature, and ratio of vapor to gas) depends on the total and vapor pressure at the inlet to the condenser, the condenser surface temperature, and the rate of heat transfer from the condensing surface.

Intergration with Thermoelectic Integrated Membrane Evaporation System

Another possible combination of evaporator type, latent heat return method and condenser/separator technique is the Thermoelectric Integrated Membrane Evaporation System (TIMES) developed by Hamilton Standard, Division of United Technologies Corporation, Windsor Locks, Conn. Figure 4 is a schematic of TIMES integrated with the dual catalyst water recovery method. In principle, the thermoelectric heat pump absorbs heat at its cold surface and dissipates it at a hotter surface. A semiconductor material provides the driving force, obtained from an electrical power source, for maintaining the temperature differential between the two surfaces. The condenser is built on the cold side of the thermoelectric heat pump and is a wet cooled porous plate which acts like a sponge absorbing the condensate which is withdrawn through the porous plate by a pump action. The hot side of the thermoelectric heat pump is utilized to heat up a relatively large rate of liquid flow which is continuously circulating through the heater and then through a hollow fiber membrane (HFM) evaporator. The liquid flow loses the heat absorbed at the heater side of the thermoelectric heat pump to the small amount of evaporating liquid at the hollow fiber membrane (HFM) evaporator.

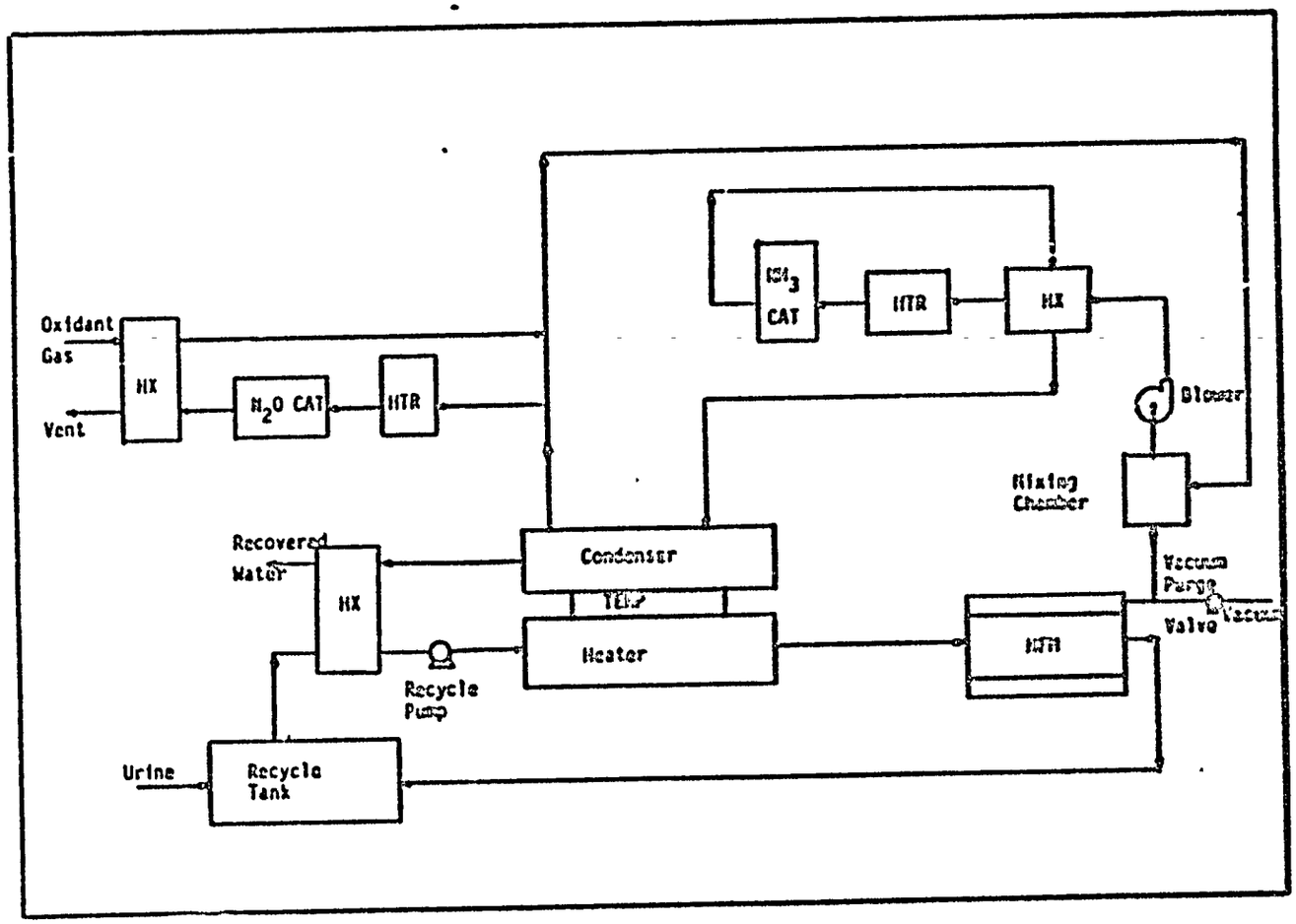

Figure 4 DUAL CATALYST INTEGRATED WITH TIMES

The resulting vapor, mixed with non-condensable gases, is withdrawn from the HFM evaporator, mixed with the oxidation gas and recycled vapor-gas mixture, and pumped through the NH_3 oxidation catalyst, then to the condenser/separator where some of it condenses and is drawn off. The rest is recycled again, after tapping off a small portion for venting through the H_2O decomposition catalyst.

Heat Transfer Calculations at the Heater.- The heat transfer rate at the heater is calculated using the experimental data for the heat transfer between parallel plates with constant but unequal plate temperatures.(3) The flow and fluid properties are calculated using the correlations reported in Reference 2. The area of heat transfer needed is determined by the number and size of thermoelectric modules which, in turn, depend on the rate of heat to be rejected from the cold side of the thermoelectric heat pump (rate of condensation) and the crefficient of performance of each module. The coefficient of performance of the thermoelectric module increases as the difference between the temperature it operates under decreases. This, in effect, restricts the evaporator pressure and hence the condenser/separator pressure. Figure 5 shows the relativeness of operating parameters of the thermoelectric heat pump. Note that for a fixed temperature differences between the cold plate and the cold source and the hot plate and the hot sink, the evaporator pressure practically determines the ΔT for the thermoelectric heat pump and hence the power input needed.

Heat Transfer Calculations at the Condenser/Separator.- As mentioned before, the vapor-gas mixture enters the condenser with a saturation temperature

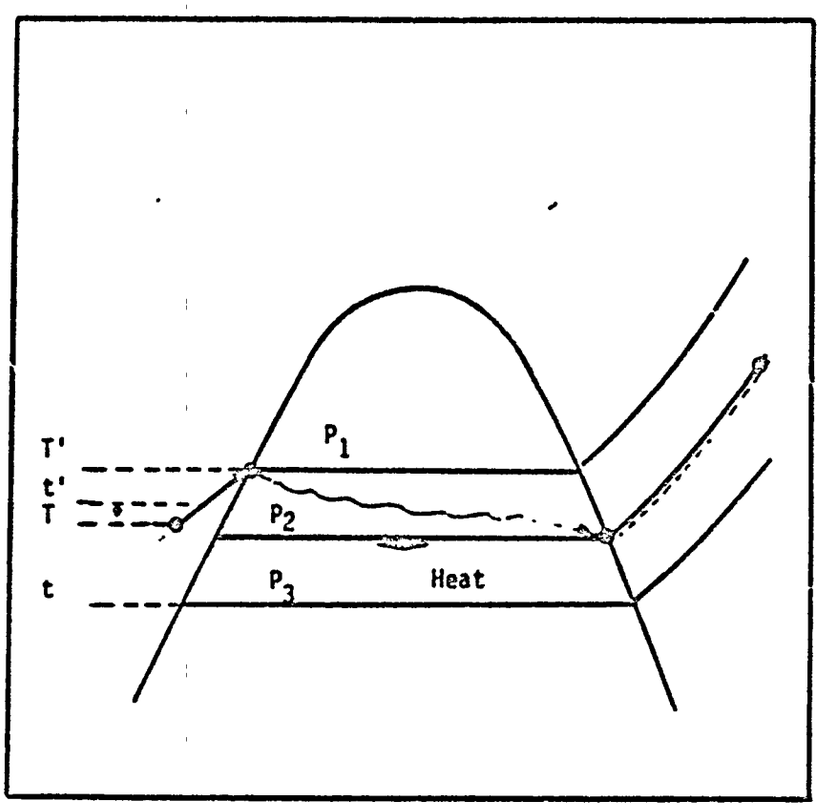

P_1 = Pressure inside the HFM

P_2 = Pressure outside the HFM

P_3 = Saturation pressure at the condenser

t = T/E cold plate temperature

t' = T/E hot plate temperature

T = bulk temperature of the liquid in the heater

T' = bulk temperature of the liquid at HFM

Figure 5 RELATION OF OPERATING PARAMETERS OF A THERMOELECTRIC HEAT PUMP

higher than the porous plate temperature. The vapor condenses under a forced convection condition. As the vapor condenses, the resulting liquid is withdrawn by a pump suction to keep the porous plate with minimum condensate film thickness. The rate of heat transfer in this process was calculated using the following expression which was experimentally verified by Kroger:[7]

$$h = \frac{q/A}{T_s - T_i}$$

$$\frac{P - P_{vi}}{W/A} \cdot \frac{D\, P_v \{h_{fg} + C_{p_v} (T_s - T_i)\}}{T_s^2\, R_g\, R_v\, (T_s - T_i)} \qquad (5)$$

where h is the coefficient of heat transfer, q is the rate of heat transfer, T is temperature, P is pressure, D is diffusivity, h_{fg} is heat of evaporation, R_g is gas constant, R_v is vapor constant, W is gas mass and A is the area of condensing surface. The subscripts i, s, and v stand for inlet, saturation, and vapor, respectively.

The maximum percentage of vapor that would condense in the condenser is also determined by the ratio between the vapor pressure at the condenser inlet and the saturation pressure set by the cold plate temperature, i.e., as the cold plate temperature decreases the condensation rate increases; however, the power input to the thermoelectric heat pump also increases with less efficiency.

It is now becoming clear that the design of the condenser/phase separator, the thermoelectric heat pump, and the heater must be matched through appropriate operating parameters for optimum results. The analytical procedure developed

carefully considers this by adjusting the rate of liquid flow in the heater-side and the temperatures selected for the thermoelectic cold and hot plates.

The Hollow Fiber Membrane (HFM) Evaporator.- The rate of evaporation per unit membrane area under the process conditions was calculated using the data reported in Reference 8, 9, and 10. For a certain flow rate, fixed fiber geometry and rate of evaporation per unit membrane area the total number of fibers is calculated as follows.

Total membrane area, $A = \dot{m}/\dot{m}_e$, (6)

where $\dot{m}$ is the intended rate of evaporation (Kg/hr) and $\dot{m}_e$ is the rate of evaporation per unit membrane area (Kg/hr m^2).

The number of fibers (n) is calculated by:

$$n = \frac{A}{\pi . D . L} , \quad (7)$$

where D and L are the fiber I. D. and length, respectively.

The power P needed to pump the urine through the hollow fiber membrane assembly is calculated as follows

$$P = \sum_{i=1}^{n} \left(\frac{1}{2} < v >^2 \frac{L}{R_h} f\right)_i + \sum_{i=1}^{n} \left(\frac{1}{2} < v >^2 e_v\right)_i \quad (8)$$

where $< v >$ = the average velocity

i = the ith fiber of n total number of fibers

L = fiber length

R_h = the mean hydraulic radius

f = friction factor

e_v = the friction loss factor

Process Thermodynamics.- An analytical procedure was developed to analyze the integrated system performance under different operating parameters. These parameters include: condenser temperature, heater temperature and temperature gradient between inlet and outlet flow, and thermoelectic heat pump operating temperature. The energy input and output is calculated for each step in the process for both of the two liquid and gas cycles. As illustrated in Figure 4, the two cycles meet in a mass transfer process in the HFH and in a heat transfer process in the thermoelectric heat pump. The effect of non-condensable gases on the rate of condensation is shown by the larger condenser area needed for a specified rate of condensate, and the larger amount of recycling mixture relative to the VCD system.

The overall specific energy input to the system is calculated by algebraically adding up the energy inputs and outputs in each subprocess. The two most important items are:

1. The power needed by the thermoelectric heat pump to transfer heat from lower temperature condensing vapor to the higher temperature liquid. The magnitude of this power heavily depends on the design and manufacturing of the thermoelectric modules. It is believed, based on consultation with different thermoelectric heat pump manufacturers and previous reports, that a coefficient of performance (COP) of value of 3 is a fairly reasonable assumption (COP is defined as the ratio of heat removed from the cold source to the work done by the thermoelectric modules.)

2. The power needed to pump the liquid through the heater and the HFM. The calculational procedure for this power is described in the previous section.

Integration with Vapor Compression/Membrane Evaporation

Previous sections discussed the integration of the dual catalyst system with known, reasonably well developed evaporation/condensation systems, namely VCD and TIMES. The main difficulties with these systems include the mechanical complexity of the VCD and the low efficiency of the thermoelectric heat pump used in TIMES.

A new concept of evaporation/condensation with heat recovery which can be integrated with the dual catalyst system for water recovery from urine was developed. This GARD concept is shown schematically in Figure 6. This concept involves the use of hollow fiber membranes for urine evaporation, a vapor compression, and a porous plate condenser, and combines the energy efficiency of the VCD with the mechanical simplicity of TIMES.

The recirculating urine passes through the heater side of the heater/porous plate condenser where its temperature is increased by the latent heat recovered from the condenser side. Fresh urine is added to the recycle stream to make-up for the portion that has been recovered as potable water, i.e. to maintain a constant volume in the recycling stream. The hot urine is then pumped through a cell of hollow fiber membrane (HFM) where a certain portion of it evaporates at the exterior surfaces of the hollow fibers, with the heat of evaporation provided by the hot fluid stream. The vapor from the HFM is mixed

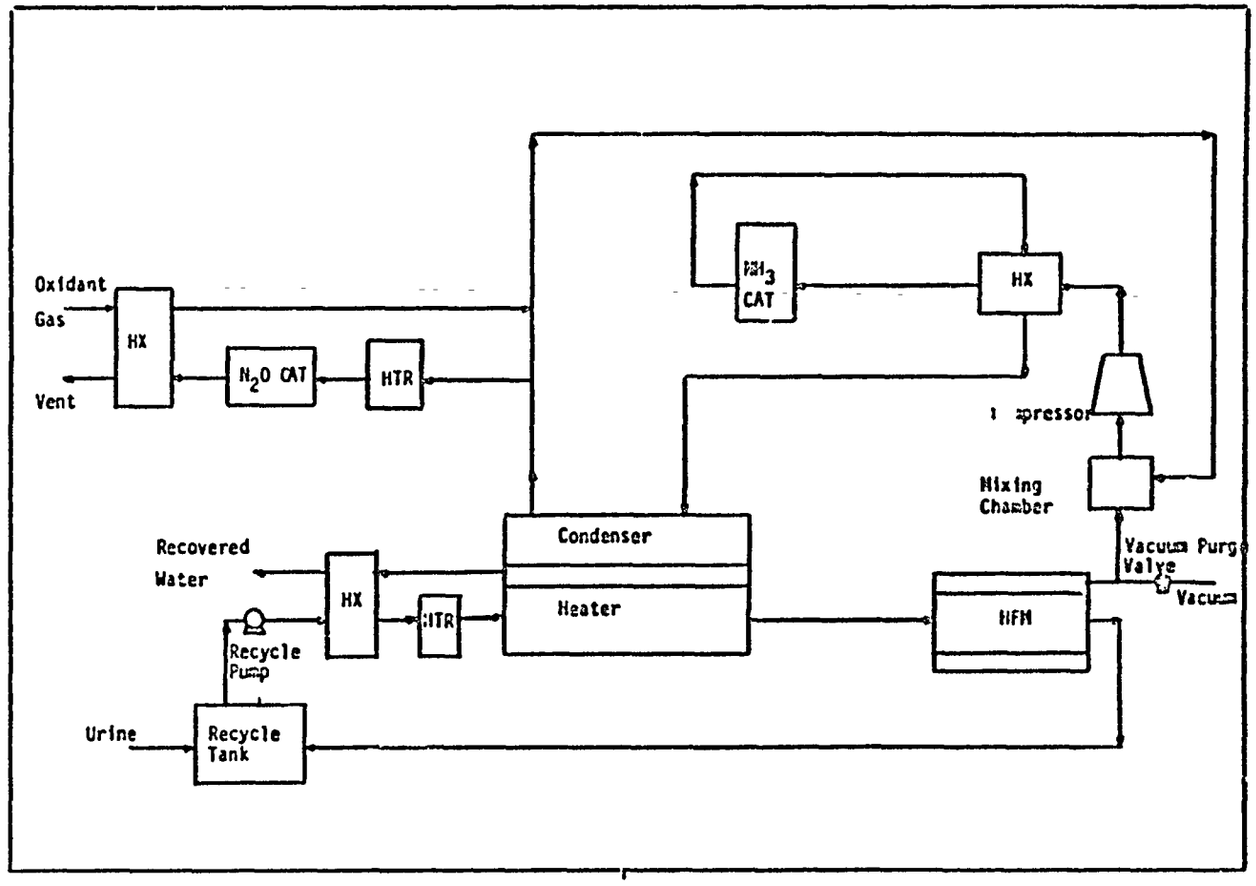

Figure 6 SCHEMATIC OF GARD SYSTEM

with the recycling vapor-gas mixture and oxidant gas, then superheated by compression to 250°C and passed directly through the NH_3 oxidation catalyst. The resulting high pressure vapor-gas mixture is then drawn into a heat exchanger to remove its superheat before it enters the porous plate condenser. The porous plate condenser is kept at a temperature below the saturation temperature corresponding to the vapor pressure of the condensing steam by the cooling effect of the recycling urine stream. The water is pumped out of the condenser and the uncondensed vapor and non-condensables mixture is recycled. A small portion of the recycled mixture is tapped off, heated to 500°C and drawn into a second catalyst where H_2O is decomposed to H_2 and O_2 and then vented to atmosphere.

The heat transfer analysis and power calculations are similar to that of VCD and TIMES. The results of these analysis are discussed in the following section.

Integration with Other Evaporative Techniques

So far, we have discussed two techniques for the evaporation process, distillation and membrane evaporation. There are other evaporative techniques that can be integrated with the dual catalyst system, such as the spray drying and flash evaporation. This section will discuss the pertinent characteristic of these evaporative methods when applied to urine water recovery in space.

Spray Dryer.- The principle of spray drying is the creation of atomizatio of a highly dispersed liquid state in a high temperature gas zone, followed by rapid evaporation and drying of the droplets. Consequently, three equally important operations are involved, namely, 1) atomization, 2) spray gas mixing

and 3) drying of liquid drops, followed by the removal and collection of dry product. Air is commonly used as the warm gas in most industrial spray dryers. In the water recovery system, however, it is desired to exclude air from the evaporative process so that the heat input is minimized and used only for vaporizing urine feed. This can be accomplished by using superheated urine vapor as the warm stream heat transport medium. Figure 7 shows a schematic of a spray drying system integrated with a thermoelectric heat pump as a condenser/ heat recovery system.

The primary advantage of the spray drying is that solids do not contact evaporator surfaces until they have become dried, which alleviates corrosion and contamination problems. Also, spray drying may frequently simplify or eliminate other operations such as filtration of the feed. The main disadvantages are its energy intensiveness and large system volume requirements because of the high gas/vapor stream temperature and flow rates required to vaporize the liquid feed.

In spray drying systems, energy is mainly consumed in:

1. Atomization of liquid. Using a pneumatic atomizer and assuming isothermal expansion, the energy Ep, needed to atomize 1 Kg of urine using W_v Kg of vapor is calculated by the following formula:

$$E_p = W_v RT \ln \frac{P_1}{P_2} . \qquad (9)$$

where

T = absolute temperature of vapor,

R = gas constant,

$\frac{P_1}{P_2}$ = pressure ratio across the atomizer.

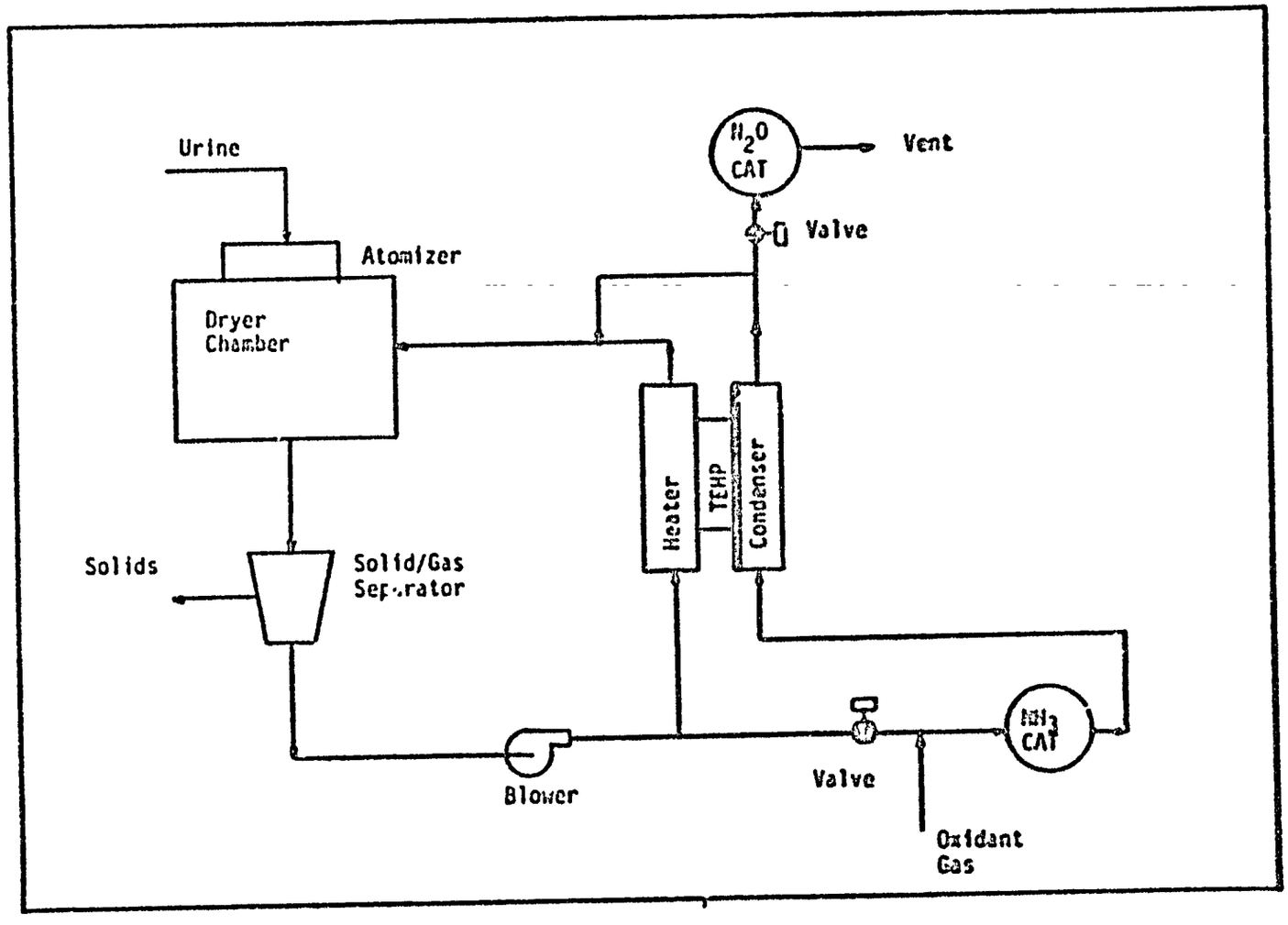
Urine
H_2O CAT
Vent
Valve
Atomizer
Dryer Chamber
Heater
TEHP
Condenser
Solids
Solid/Gas Separator
Blower
Valve
NH_3 CAT
Oxidant Gas

W_v is calculated from a heat balance equation assuming perfect mixing and inlet conditions for both liquid and vapor streams. Let the liquid inlet temperature and pressure be T_l and P_l, respectively, and ΔT the superheat of vapor, then

$$\dot{m}_e h_{fg} + \dot{m}_e \quad P_c (T_{sat} - T_e) = W_v Cp_v \Delta T, \qquad (10)$$

where $\dot{m}_l$, C_p, h_{fg} are evaporated liquid mass rate, heat capacity, and heat of evaporation at T_{sat}, respectively; T_{sat} is the resulting vapor temperature and Cp_v is the vapor heat capacity. The value of W_v obtained in Eq. 10 is then used in Eq. 9 to calcuate the energy requirement.

2. Pumping of the continuously cycling vapor used for the evaporation of the atomized urine. For a three-man system, the volumetric flow of this vapor is calculated to be in the order of 150 m^3/hr. at T = 373 K, depending on the pressure ratio across the expansion valve in the vapor line entering the spray drying chamber and, consequently, on the allowable vapor temperature drop.

3. Thermoelectric heat pump. The power consumed by the thermoelectric heat pump to transfer the heat of condensation of the condensing vapor to superheat the circulating vapor used in spray drying is considerably large. This is due to the low efficiency encountered by the gaseous heat sink which necessitates high temperature gradient and hence high difference between the thermoelectric operating temperature. Moreover, the heat transfer area needed would be larger than that needed if liquid cooling is used.

4. Solid-gas separator. Some kind of rotary equipment must be used to provide for the separation of dried solids from the vapor-gas mixture when operating under zero-gravity conditions. In addition to the design complication in satisfying this requirement, extra power consumption, weight and volume must be considered.

Because of the high power requirements and large weight and volume penalties, the spray drying concept is deemed unsuitable for space applications

Flash Evaporation.- The flash evaporation, as illustrated in Figure 8, is a process in which the preheated liquid is pumped into a reduced pressure vessel. The sudden expansion produces vapor at the expense of liquid. The process occurs adiabatically due to the fast rate of heat transfer needed in the evaporation. The mixture of vapor, gas, and liquid is then introduced into a gas-liquid separating vessel which, in zero gravity environment, requires carefully arranged rotary motion to generate centrifugal forces to separate liquid droplets from gas. Similarly to TIMES, the flash evaporation method provides for separate evaporation and heating processes, and a form of heat pumping device (thermoelectric or auxiliary vapor cycle) is needed. However, added design complications and energy consumption in the vapor-liquid separation process make it unfavorable.

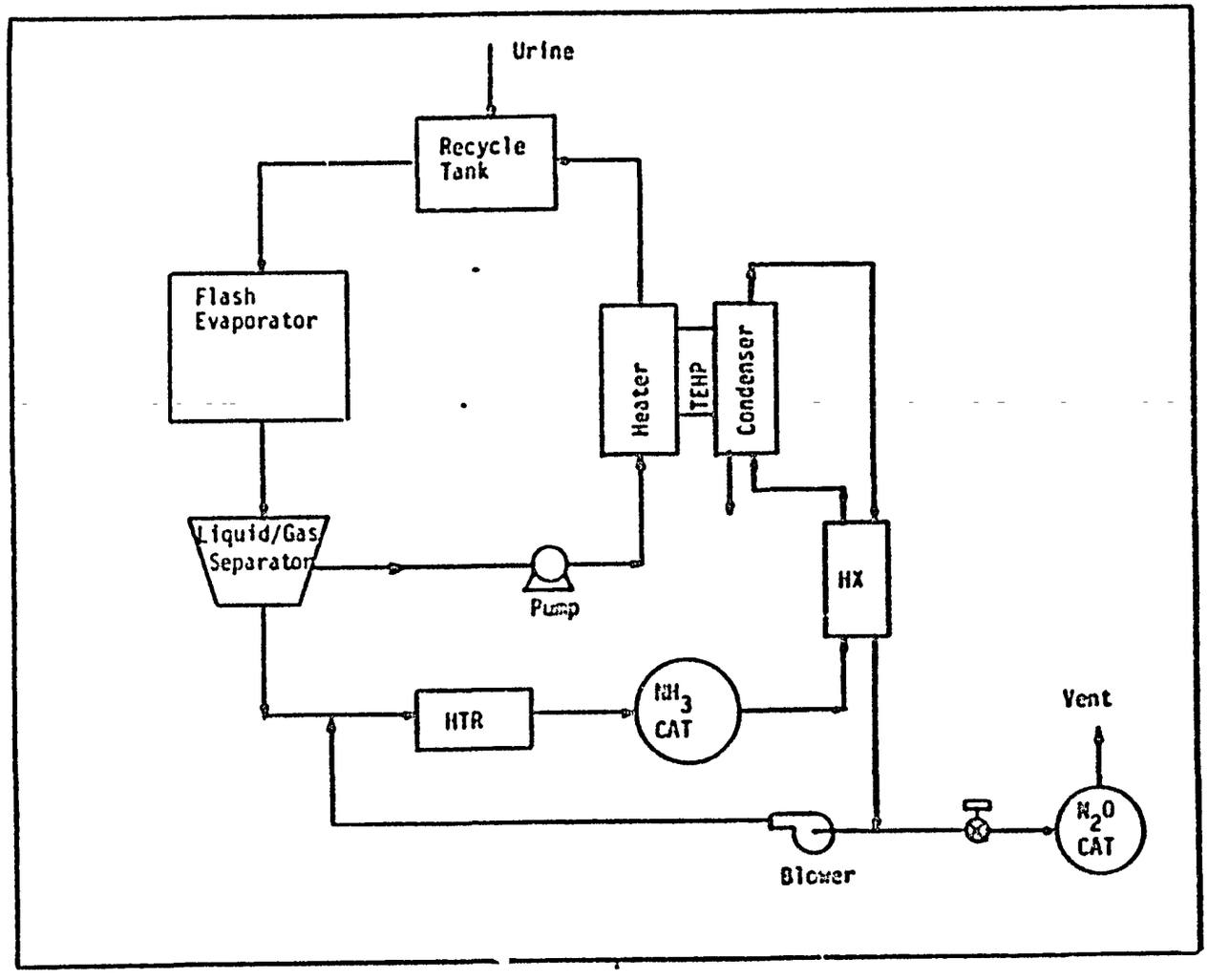

Figure 8 FLASH EVAPORATOR INTEGRATED WITH DUAL CATALYST SYSTEM

ENERGY REQUIREMENTS

Energy requirements for water recovery systems based on catalytic treatment of urine vapor integrated with the three feasible methods of evaporation/condensation were calculated using thermodynamic and heat transfer consideration discussed in the previous section. To provide a meaningful comparison, the calculations were performed in the same manner for all three systems by using common basic parameters and adding only those parameters that are specific for each system. The basic input parameters common to every system are: operating temperatures of the catalysts, potable water mass rate, percent of oxygen required for achieving ammonia oxidation, percentages of CO_2, H_2O and O_2 in the recycled vapor/gas mixture, conditions in the evaporator/condenser, and physical properties. The values of the basic input parameters are listed in Table 1.

The following assumptions were used:

1. A fixed rate of potable water production,
2. Perfect thermal insulation,
3. Perfect heat exchange.

The calculations considered the path of the process and determined the required energy and the available energy at various points; however, no attempt was made to determine in which manner the available energy should be best utilized. All the available heat was considered a credit during the calculations (i.e., a perfect heat exhange); however, a correction assuming

TABLE 1 BASIC INPUT PARAMETERS

Temperature at oxidation catalyst, °C	250
Temperature at decomposing catalyst, °C	500
Inlet temperature of urine, °C	25
Inlet temperature of oxidant, °C	25
Exit temperature of liquid, °C	25
Exit temperature of vent gas, °C	300
Urine mass flowrate, Kg/hr	0.854
Solids in urine, %	15
Oxygen, %	6
Carbon dioxide, %	4
Nitros oxide, %	3
Heat capacity of liquid, KJ/Kg°C	4.20
Heat capacity of vapor, KJ/Kg°C	2.04
Heat capacity of gas, KJ/Kg°C	1.04

an 85% efficiency of the heat exchanger was applied to the final energy requirement value. Although this method introduces a certain error in the calculated values of specific energy requirements, it provides a meaningful comparison of the three systems as long as each of them is treated in the same manner.

GARD System

Evaporation.- The area of the heater was calculated by assuming a fixed distance between the parallel plates and a fixed temperature difference between wall and the liquid bulk temperatures. The following relation was used to calculate the heat transfer coefficient:

$$Nu = 33.316 + 6.918\ Pr,$$

where Nu and Pr are Nusselt and Prandtl numbers, respectively. Based on the heat transferred from the condenser, the heater area was calculated. The recycling fluid flow rate was determined assuming a maximum temperature rise for the fluid flowing through the heater.

The heated urine passes through a hollow fiber membrane evaporator module where water vapor diffusing through the tube wall evaporates at the outside surfaces of the fibers, and the heat of evaporation is provided by the hot urine stream. The liquid pump power requirement was calculated on the basis of assumed total area of the hollow fiber membrane with known specifications (length, diameter).

Vapor Cycle Calculations.- The polytropic process relation for the ideal gases was used to calculate the only unknown condition across the compressor,

i.e., exit pressure; then the compression flow work was calculated based on a motor/compressor mechanical efficiency of 0.8.

The vapor-gas mixture enters the condenser at a saturation temperature higher than the condenser temperature and condenses under a forced convection condition. As explained earlier, the maximum percentage of vapor that would condense in the condenser was determined by the ratio between the vapor pressure at the condenser inlet and the saturation pressure at the condenser.

Calculated Energy Requirement.- Several computer runs were made for the GARD System at evaporation temperatures of 90°, 80°, and 60°C, and different condensation temperatures. The results are summarized in Table 2 and Figure 9. The calculations indicate that, for a given evaporation temperature, the required specific energy increases with an increase in the condensation temperature. This behavior can be explained by realizing that an increase in the condensation temperature decreases the available heat of condensation; therefore, less energy is transferred to the recycling liquid. Because the required heat of evaporation is fixed for each specific evaporation temperature and rate, additional energy must be provided externally to offset the decrease in the available heat of condensation. On the other hand, the power consumption of the liquid pump becomes lower at higher condensation temperatures; however, the net result is higher overall energy requirement.

As shown in Figure 9, raising the evaporation temperature has a favorable effect on the energy requirement of the system at any given condensation temperature. Lowering specific energy requirements at higher evaporation

TABLE 2 ENERGY REQUIREMENTS FOR GARD SYSTEM

Evaporation Temperature, °C (°F)	Condensation Temperature, °C (°F)	Oxidizing Gas, 6% O_2	Specific Energy, KJ/Kg ($\frac{Watt - hr}{lb}$
60 (140)	65 (149)	Oxygen	564.4 (71)
60 (140)	70 (158)	Oxygen	570.1 (71.7)
60 (140)	75 (167)	Oxygen	577.2 (72.6)
60 (140)	80 (176)	Oxygen	585.5 (73.6)
60 (140)	85 (185)	Oxygen	594.6 (74.8)
80 (176)	85 (185)	Oxygen	560.7 (70.5)
80 (176)	90 (194)	Oxygen	567.1 (71.3)
80 (176)	95 (203)	Oxygen	575.1 (72.3)
80 (176)	100 (212)	Oxygen	584.8 (73.5)
95 (203)	100 (212)	Oxygen	556.4 (69.9)
95 (203)	105 (221)	Oxygen	566.3 (71.2)
95 (203)	110 (230)	Oxygen	573.6 (72.1)
95 (203)	115 (239)	Oxygen	585.7 (73.6)
95 (230)	120 (248)	Oxygen	593.4 (74.6)
80 (176)	85 (185)	Air	707.4 (88.9)
80 (176)	90 (194)	Air	716.3 (90.1)
80 (176)	95 (203)	Air	727.2 (91.5)
80 (176)	100 (212)	Air	739.0 (93)

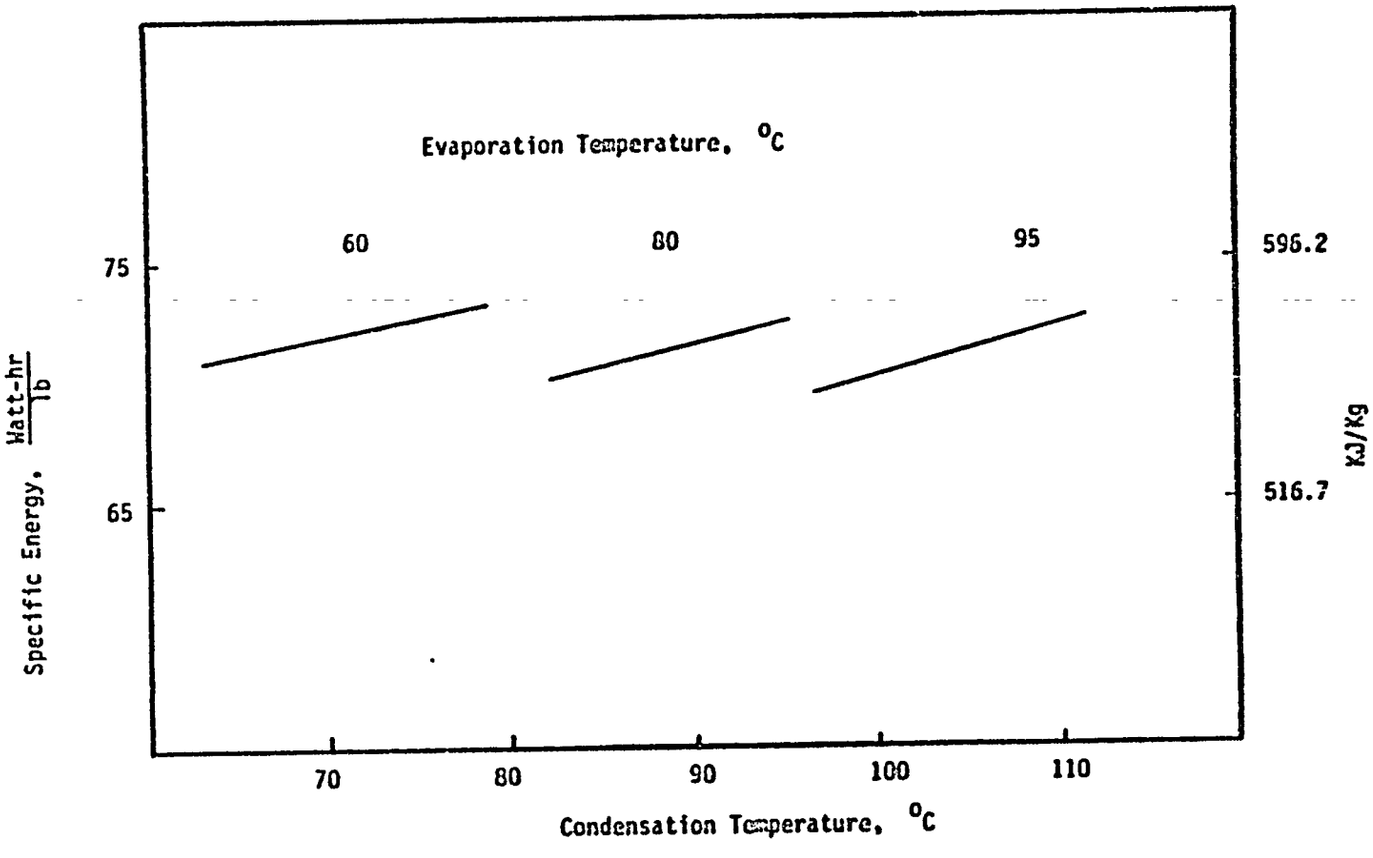

Figure 9 ENERGY REQUIREMENTS FOR GARD SYSTEM

temperatures at a given condensation temperature can be attributed to the following factors:

1) At higher evaporation temperatures, raising the temperature of the vapor-gas mixture stream to 250°C by compression requires less compressor work.

2) At higher evaporation temperature more vapor can be condensed due to the higher pressure difference between the vapor stream entering the condenser and the equilibrium at the condenser surface.

The analysis indicates that the energy requirement of the GARD System is lower than that of TIMES (as used today, i.e., without a catalytic vapor treatment), mainly because of the elimination of the thermoelectric heat pump. This encouraging result indicates that the GARD system is a promising concept that can be used to provide potable water from urine at an efficiency higher than TIMES but with a similar mechanical simplicity.

When air is used as the oxidizing gas instead of oxygen, the energy requirement is higher than that required with oxygen.

Integration with TIMES

Liquid and vapor cycles were analyzed in the same way as described for the GARD System, except for the thermoelectric heat pump and for a minor change in the heater calculations. The coefficient of performance (COP) of four (4) was used to evaluate the power requirement of the thermoelectric

heat pump, although such a high COP might not be attainable at large temperature differentials. In the parallel plate heater calculations, the area is fixed for the conditions studied instead of fixing the distance between the two plates.

To check the accuracy of the computer program, a run was made for the TIMES system by modifying some parts of the program and using conditions similar to those reported by Winkler and Roebelen[10] and summarized in Table 3. They report that the energy requirement under these conditions is about 108 W-hr/lb. The required specific energy obtained by our calculations is 132 W-hr/lb., which is reasonably close to the value reported by Winkler and Roebelen.

Table 4 and Figure 10 show the required specific energies for the system integrated with TIMES at various operating conditions. It can be seen that the specific energy requirement of the system is higher than the GARD System, and follows a different trend. At a given evaporation temperature, the required specific energy decreases with an increase in the condensation temperature. Since the system operates at a constant ΔT in the condenser, the liquid pumping rate, the rate of heat transfer by the thermoelectric element and the direct heating must be balanced. Although each of these parameters changes differently with the temperature of condensation, the net result is a lower energy requirement at higher condensation temperatures. For the same reasons explained for the GARD System, raising the evaporation temperature results in lower energy requirements.

TABLE 3 TIMES OPERATING CONDITIONS

Potable water mass rate, Kg/hr	0.771
Condensation temperature, °C	57
The hot junction temperature, °C	66
Coefficient of performance	4
Hollow fiber membrane (HFM) I.D., cm	0.05
Total available area of HFM, cm^2	3678

TABLE 4 ENERGY REQUIREMENTS OF SYSTEM INTEGRATED WITH TIRES

Evaporation Temperature, °C (°F)	Condensation Temperature, °C (°F)	Oxidizing Gas, 6% O_2	Specific Energy, kJ/kg ($\frac{Watt - hr}{lb}$)
60 (149)	27.5 (81.5)	Oxygen	1356.2 (171.8)
60 (149)	30 (86)	Oxygen	1350.8 (171.2)
60 (149)	32.5 (90.5)	Oxygen	1355.9 (170.6)
85 (185)	47.5 (117.5)	Oxygen	1331.5 (167.5)
85 (185)	50 (122)	Oxygen	1324.2 (166.6)
85 (185)	52.5 (126.5)	Oxygen	1318.9 (165.9)
95 (203)	55 (131)	Oxygen	1315.9 (165.5)
95 (203)	57.5 (135.5)	Oxygen	1310.6 (164.8)
95 (203)	60 (140)	Oxygen	1304 (164.0)

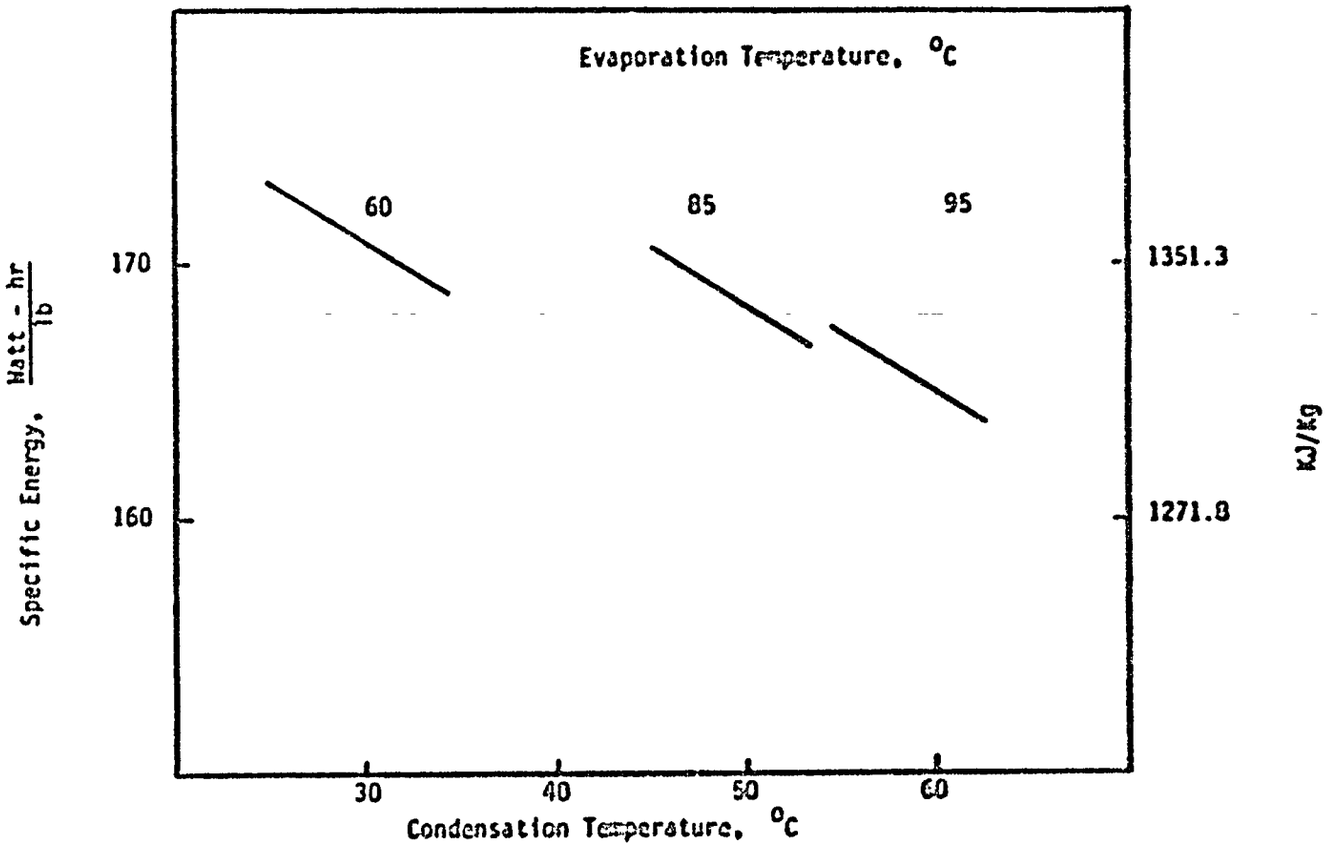

Figure 10 ENERGY REQUIREMENTS FOR SYSTEM INTEGRATED WITH TIMES

Integration with VCD

The energy requirements for a dual catalyst system integrated with VCD was calculated in a manner similar to the two other systems. Generally, the VCD energy requirements can be subdivided into a specific energy of the process and a mechanical hardware energy. Since the energy required for hardware components such as centrifuge motor for rotating evaporator/condenser, solenoid valves, and fluid pumps were not included in the computer program, a fixed value of the hardware energy was added for obtaining the final results. Thompson et al[12] estimate the process hardware energy for their system at 25.3 Watt-hr/lb.

The area of the evaporator was calculated using Eq. 1 and assuming the temperature of the evaporator wall to be an average of the temperature of evaporation and condensation. The heat transfer rate in the condenser was calculated using Eqs. 2 through 4 and then correcting for the effect of non-condensables.

The results for several operating conditions are summarized in Table 5. Figure 11 displays the effect of changing the evaporation and condensation temperatures on the specific energy requirement of the system. Similarly to the GARD System, increasing the condensation temperature increases the energy requirement. This can be explained by noting that an increase in the condensation temperature results in a higher partial pressure of water vapor leaving the condenser, i.e., more vapor in the recycle stream that has to be recycled and recompressed. The higher energy requirement of the system at higher evaporation temperature can be explained by realizing that more energy is required to preheat the feed.

TABLE 5 ENERGY REQUIREMENTS OF SYSTEM INTEGRATED WITH VCD

Evaporation Temperature, °C (°F)	Condensation Temperature, °C (°F)	Oxidizing Gas, 6%	Process Specific Energy, KJ/Kg ($\frac{Watt - hr}{lb}$)	Total Specific Energy, KJ/Kg ($\frac{Watt - hr}{lb}$)
60 (140)	65 (149)	Oxygen	271.9 (34.2)	471.7 (59.3)
60 (140)	70 (158)	Oxygen	283.3 (35.6)	483.1 (60.9)
60 (140)	75 (167)	Oxygen	295.5 (37.1)	495.3 (62.4)
80 (176)	85 (185)	Oxygen	367.9 (46.3)	567.7 (71.6)
80 (176)	90 (194)	Oxygen	330.2 (47.8)	580 (73.1)
80 (176)	95 (203)	Oxygen	393.6 (49.5)	593.4 (74.8)
90 (194)	95 (203)	Oxygen	415.5 (52.2)	615.3 (77.5)
90 (194)	97 (207)	Oxygen	420.9 (52.9)	620.7 (78.2)
90 (194)	100 (212)	Oxygen	428.5 (53.9)	628.3 (79.2)

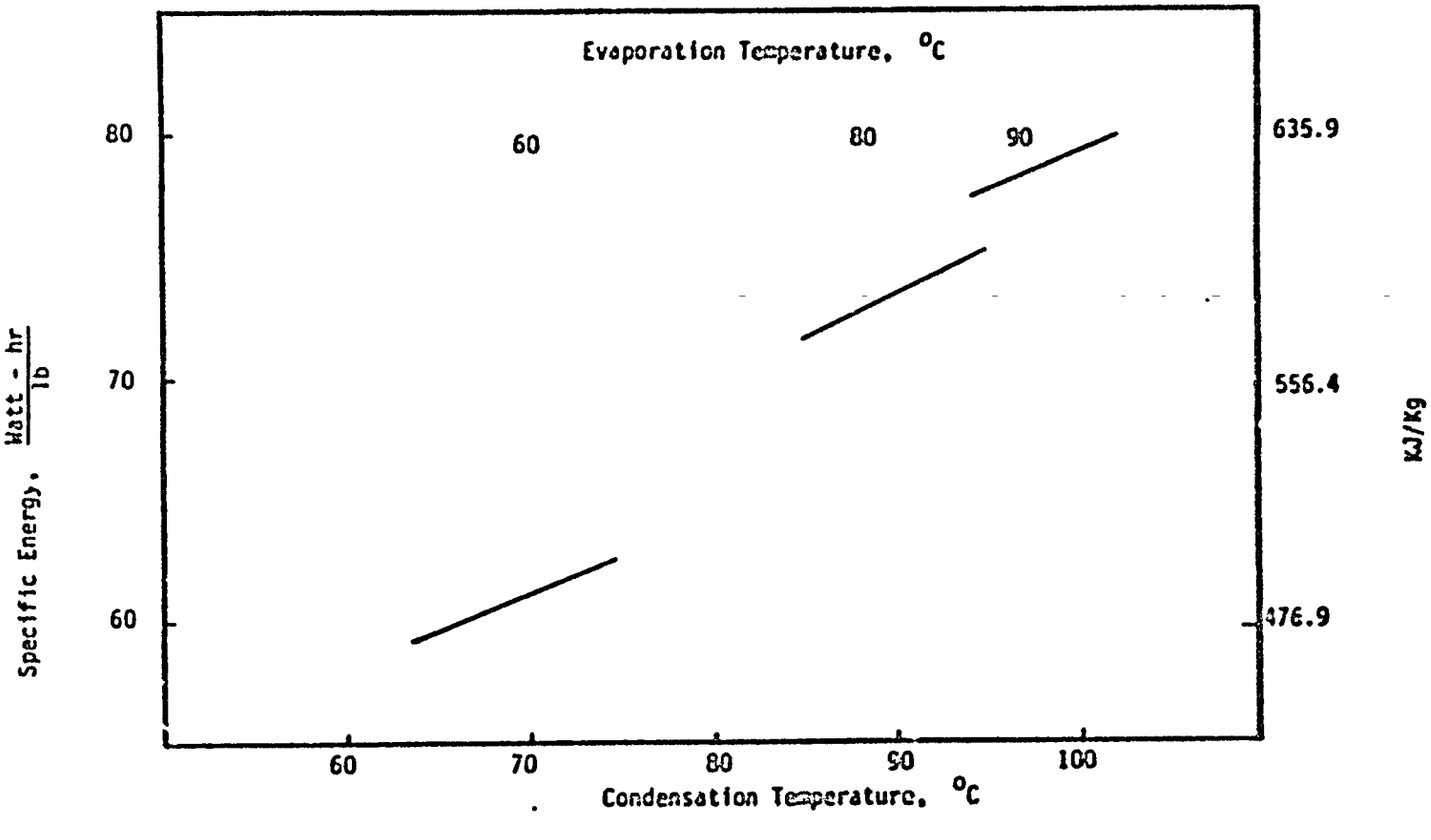

Figure 11 ENERGY REQUIREMENTS FOR SYSTEM INTEGRATED WITH VCD

Comparison of the Systems

The results of the most energy efficient cases of the three systems are presented in Table 6. In this Table, in addition to the specific energy calculated assuming a complete recovery and utilization of the available energy, the energy requirements using heat exchange of 85% efficiency are also indicated. The system with the lowest energy requirements utilizes VCD for the evaporation/condensation and heat recovery. However, this system entails the mechanical complexity of the VCD and the difficulties of liquid film handling on a rotating drum.

The system utilizing TIMES has the highest energy requirements, mainly because of the low efficiency of the thermoelectric heat pump; however, this system has no moving parts other than pumps and is, therefore, mechanically simple.

The calculated energy requirements for the GARD System are somewhat highe compared with a system utilizing VCD but significantly lower compared with a system integrated with TIMES. Actually, the GARD system requires less energy than the TIMES system presently under development which does not include any catalytic treatment. The GARD concept can be regarded as a hybrid employing desirable and rejecting undesirable features of both VCD and TIMES. It avoids the mechanical complexity of the VCD and the poor efficiency of the thermoelectric heat pump. Its main components (hollow fiber evaporator, vapor compression, porous plate condensation) have been previously, sufficiently tested in other systems.

TABLE 6 COMPARISON OF THE MOST EFFICIENT CASES OF THE THREE SYSTEMS

SYSTEM	Evaporation Temperature, °C (°F)	Condensation Temperature, °C (°F)	Oxidizing Gas, 6% O_2	Specific Energy, KJ/Kg ($\frac{Watt - hr}{lb}$)	Energy with 85% Heat Exchanger Efficiency, KJ/Kg ($\frac{Watt - hr}{lb}$)
Dual catalyst system integrated with VCD	60 (140)	65 (149)	Oxygen	471.7 (59.3)	591.4 (74.4)
Dual catalyst system integrated with THES	95 (203)	60 (140)	Oxygen	1304 (164)	1570.3 (197.5)
GARD System	95 (203)	100 (212)	Oxygen	555.4 (69.9)	659.6 (85.7)

It should be kept in mind that the calculated values presented here constitute only the calculated energy requirements of these systems. A design study is necessary to obtain the best configurations and the actual weight and volume penalties; however, weights and volumes of the three systems considered here can be assumed to be close to each other.

CONDENSER DEVELOPMENT AND TESTING

Based on the analytical evaluation of various conceptual systems for integrated water recovery by the dual catalyst method described in previous sections, a concept utilizing a porous plate for condensing the recovered water with a direct heat exchange to feed urine was found the most promising. Such a condenser must be suitable for

1. Operation under zero-g conditions,
2. Condensation of recovered water from superheated steam containing up to 20% of noncondensable gases entering the condenser at temperatures ranging up to 250°C,
3. Recovery and transfer of the heat of condensation to feed urine.

Although the recovery/removal of water vapor on porous plates has been investigated and used before, little data are available that are applicable to this particular application. Therefore, the development of the condenser was pursued in three stages:

1. Construction and testing of a flat plate condenser for the purpose of obtaining heat transfer and condensation efficiency data,
2. Design and fabrication of a cylindrical condenser suitable for integration with a three-man catalytic water recovery system,
3. Testing of the cylindrical condenser first with steam, then integrated with the dual catalyst system.

Flat Plate Condenser

Description.- The flat plate condenser and its components are shown in Figures 12 and 13. The central piece of assembly is a 25.4 cm (10") long, 22.9 cm (9") wide and 0.32 cm (0.125") thick aluminum base plate. A porous plate, 15.2 cm (6") long, 15.2 cm (6") wide, and 0.32 cm (0.125") thick, of a 40% dense sintered fiber copper having a nominal permeability of 0.95 L/min-m^2-Pa (160 gal.min-ft^2-Psi) for water and dry thermal conductivity of 10.2 watt:/m -°C (5.9 Btu/hr-ft-°F) was installed on the condensing side of the baseplate in a way allowing a 0.1 cm (0.04") gap between the plates for passage of the condensed water. The other side of the base plate is exposed to the cooling water and contains 12 aluminum pins spaced 2.54 cm (1") apart in a square pitch arrangement for increasing the heat transfer. A stainless steel tube of 0.95 cm (0.375") I.D. is connected to a hole located in the center of the base plate for withdrawal of the condensed water accumulating in the gap between the base plate and the porous plate. Both sides of the base plate are covered with enclosures constructed from a clear 0.95 cm (0.375") thick polycarbonate plate, with rubber gaskets placed between the base plate and the enclosures for a leak-tight seal. The polycarbonate enclosures allow a visual observation of the condensation process. The enclosure covering the porous plate contains ports for steam inlet and outlet and baffles near steam entrance and exit for achieving a uniform steam distribution. The coolant side enclosure has an inlet and outlet for cooling water. Chromel-Alumel thermocouples are installed to monitor the temperature of inlets and outlets for steam and water and also the surface temperature of the base plate.

ORIGINAL PAGE
BLACK AND WHITE PHOTOGRAPH

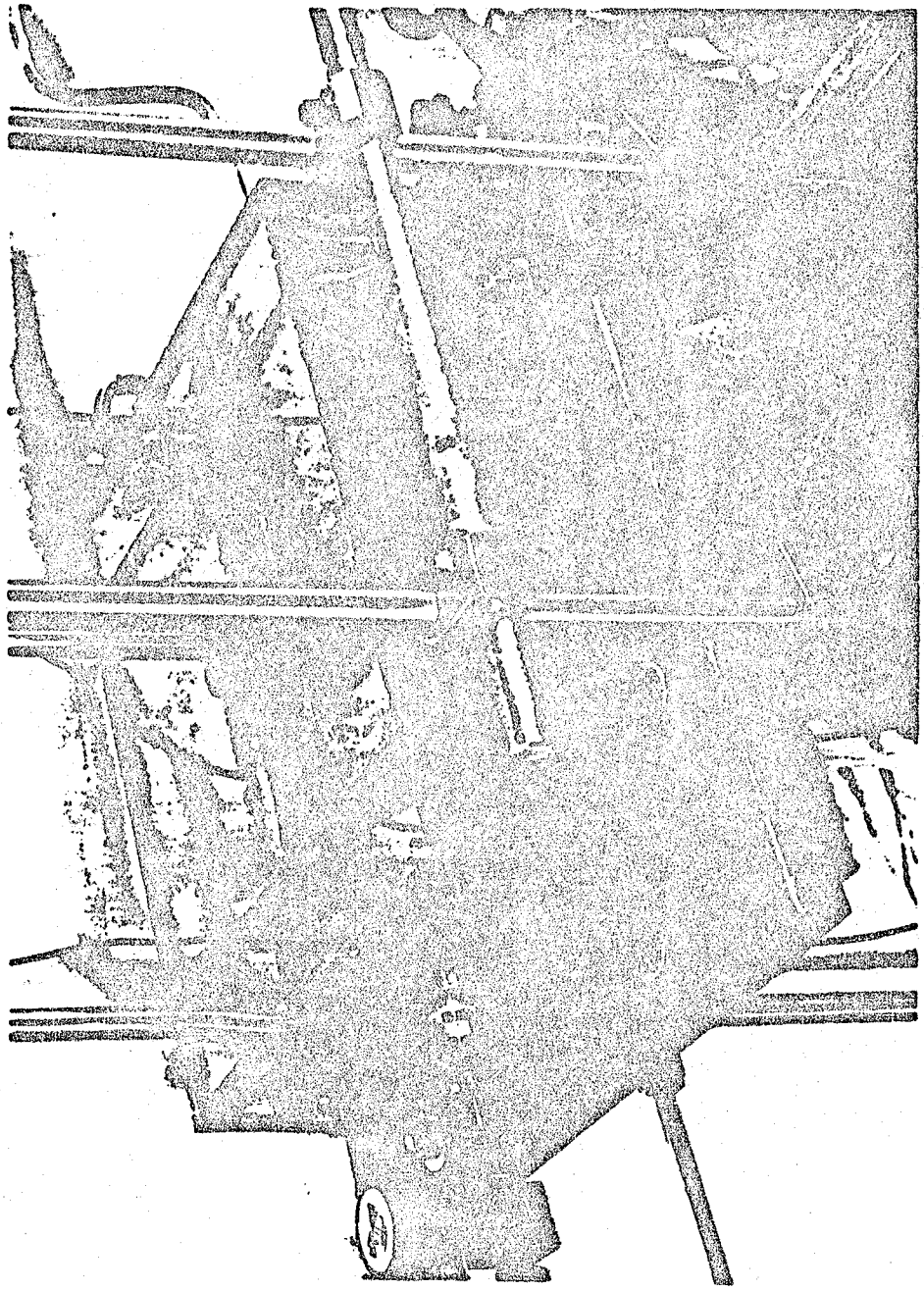

Figure 12 FLAT PLATE CONDENSER

ORIGINAL PAGE
BLACK AND WHITE PHOTOGRAPH

Figure 13 COMPONENTS OF THE FLAT PLATE CONDENSER

Experimental Set-up.- The flat plate condenser was tested in an experimental arrangement shown in Figure 14. Steam was generated from distilled water at atmospheric pressure in a glass boiler heated by an electric heating mantle whose electrical input was regulated by a variable transformer. Steam was mixed with measured amounts of air, then delivered to the condensing side of the flat plate condenser. The condensate collected by the porous plate was removed by a slight vacuum applied to the condensate collector. Vapor remaining uncondensed and leaving the condenser with the air stream was removed and collected by an auxiliary condenser maintained at approximately 21.1°C (70°F). The flowrate of the coolant water was measured by a flowmeter, then it was preheated to a desired temperature by passing through a copper coil immersed in a constant temperature bath. The system was started and allowed to achieve a steady state which was indicated by a constant outlet temperature of the coolant water, then the test was initiated and continued for one hour.

During the preliminary testing, it was observed that there was some condensation on the upper enclosure of the condenser resulting in water droplets falling on the porous plate and, thus, giving erroneous results. The problem was eliminated by additional insulation and by operating the condenser upside down, so that any condensate formed on the walls did not reach the porous plate.

Test Results.- Tests were performed first with steam alone, then with a mixture of steam and air. Both types of tests were repeated with coolant water at 21.1°C (70°F), 52.2°C (135°F), and 65.5°C (150°F). The results of these tests are summarized in Table 7.

ORIGINAL PAGE
BLACK AND WHITE PHOTOGRAPH

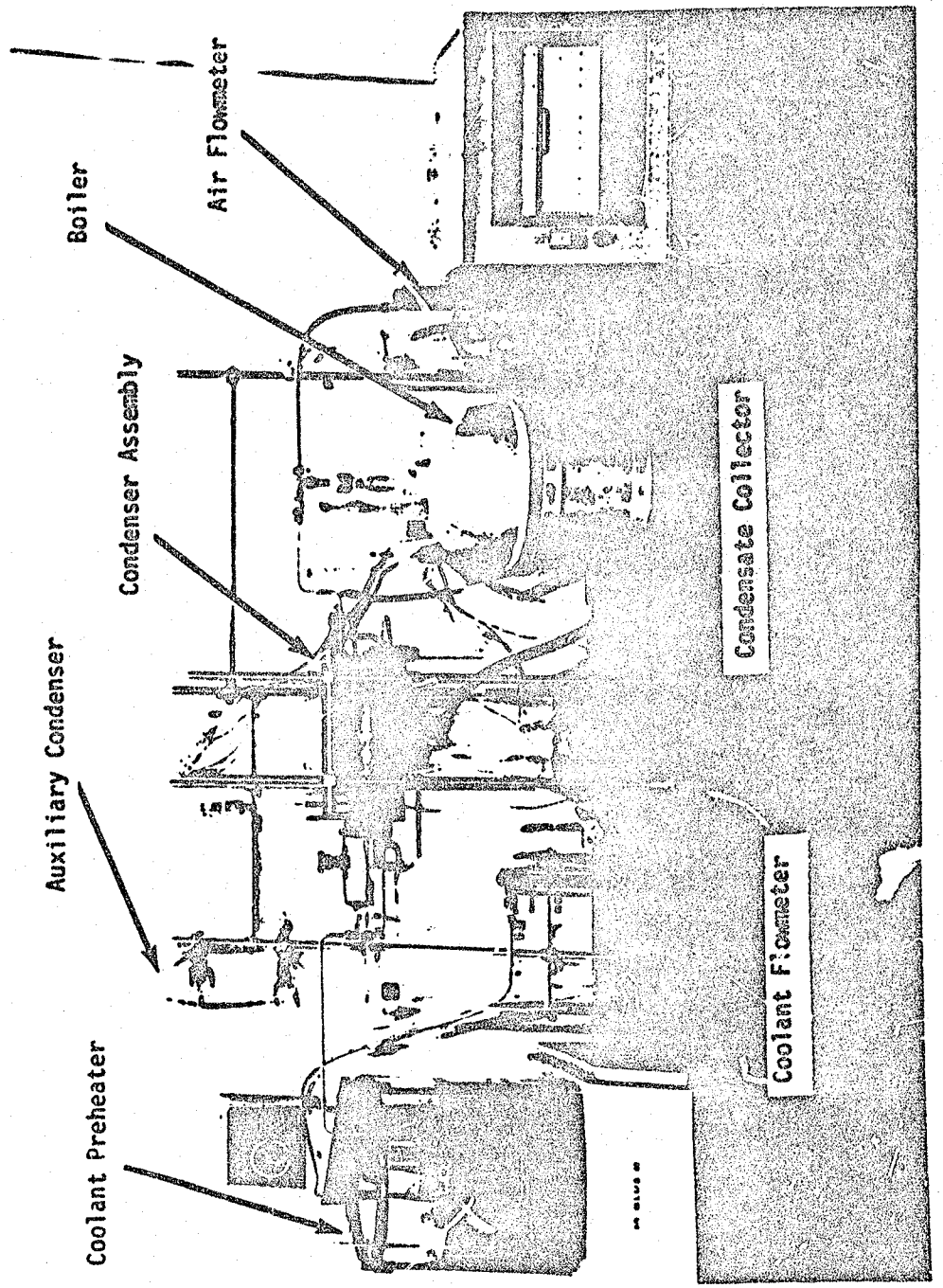

TABLE 7 FLAT PLATE CONDENSER TEST RESULTS

Run No	FEED		COOLANT			CONDENSER							
	Steam, gr/hr	Air, L/hr	Flow-Rate, ml/min	Temperature, °C		Heat Transfer Rate, KJ/hr		Temperature, °C		Recovered Water, gr/hr	Uncondensed Vapor, gr/hr		Condenser Efficiency, %
				Inlet	Outlet	Actual	Theoretical	Inlet	Outlet		Actual	Theoretical	
1	763	2.4	1040	21.1	27.2	1595	1702	101.1	100.0	600	83	Negl.	80
2	790	2.4	1160	57.2	62.2	1433	1703	101.1	100.5	700	50	Negl.	89
3	709	2.4	1040	65.5	70.0	1155	1345	101.6	100.0	554	155	Negl.	78
4	774	300	990	21.1	25.5	1092	1265	102.2	51.1	481	293	6	63
5	768	300	1010	57.2	60.5	823	977	101.6	82.8	397	371	50	55
6	779	300	1010	65.5	68.3	693	921	101.6	83.9	324	326	81	55

The feed rate to the condenser was calculated by adding the measured quantities of water recovered by the porous plate, condensing on the wall of the enclosure, condensed by the auxiliary condenser, and leaving with the vent air. The condenser efficiencies for various coolant temperatures were calculated by determining the ratio of the recovered water to the maximum possible recovery, expressed by the difference between the feed and the calculated amount of vapor leaving the condenser with air at saturation. The low efficiencies of the flat plate condenser are mainly due to a small porous plate area and condensation on the enclosure walls.

The amount of heat gained by the coolant, i.e., the heat transfer rate, was determined from the coolant flowrate and temperature rise. The theoretical rate of heat transfer from the condensation side to the coolant side was calculated by making an overall heat balance across the condenser. The flux to the coolant side is the sum of latent heat of condensation and sensible heat recovered from the gas phase due to temperature difference between the gas phase and the condensation temperature. On the average, the experimental rate of heat transfer for the flat plate condenser is 84% of the theoretical value.

The average overall heat transfer coefficient, U, for the composite condenser assembly based on the porous plate area was calculated to be 277 watt/m^2-°C. This heat transfer coefficient was used in estimating the heat transfer parameters for the design of a cylindrical three-man condenser.

Cylindrical Condenser

Design Considerations.- Condensation from a vapor-gas mixture does not occur at nearly constant temperature as in the case for pure vapor.

Instead, due to the change in the mass ratio of vapor and noncondensable gas, the temperature decreases as the mixture progresses through the condenser. To accurately model this condensation process, it is necessary to use a stepwise numerical analysis, i.e., one in which the length of the condenser is divided into a series of finite elements. It is also necessary to consider the variation of local thermodynamic properties and their effect on the local heat and mass transfer coefficients for each finite element. One method of condenser design which satisfies the above requirements is the Colburn and Hougen[13] technique.

A three-man capacity condenser was designed using the Colburn-Hougen technique and using design factors summarized in Table 8. Since a cylindrical tube and shell type configuration provides larger surface area per unit volume than a flat configuration, a cylindrical shape was selected. The optimum surface area of the porous plate is obtained with steam flowing on the shell side and cooling liquid on the tube side. Convenient diameters of shell and tube were selected on the basis of commercial availability of stainless steel tubing, then the length required for obtaining the necessary surface area was calculated. Table 9 shows dimensions of the condenser components.

Description.- Figures 15 and 16 show the schematic and the actual condenser assembly, Figure 17 presents its components, and Figure 18 its cross section. The inner tube and the outer jacket are fashioned from commercially available thin wall stainless steel tubing, while the porous tube was constructed by rolling a porous copper sheet and silver brazing the sides together. The specifications of porous sheet are identical to those used in the flat plate condenser. Steam is introduced tangentially

TABLE 8 DESIGN CONDITIONS FOR A THREE-KW! CAPACITY CONDENSER

Water Recovery Rate, gr/hr	915
Feed Rate	
Steam, gr/hr	990
Air, L/hr	311
Condenser	
Inlet Temperature, °C	104
Outlet Temperature °C	65
Coolant Liquid	
Flow Rate, ml/min	1178
Inlet Temperature, °C	54
Outlet Temperature, °C	60
Operation Time, hrs/day	16

TABLE 9 DESIGN DIMENSIONS OF THE CYLINDRICAL CONDENSER

Porous Tube	
Surface Area, cm^2	883
Inside Diameter, cm	4.95
Outside Diameter, cm	5.59
Length, cm	50.3
Inner Tube	
Inside Diameter, cm	4.42
Outside Diameter, cm	4.75
Outer Jacket	
Inside Diameter, cm	6.09
Outside Diameter, cm	6.35
Length, cm	50.9

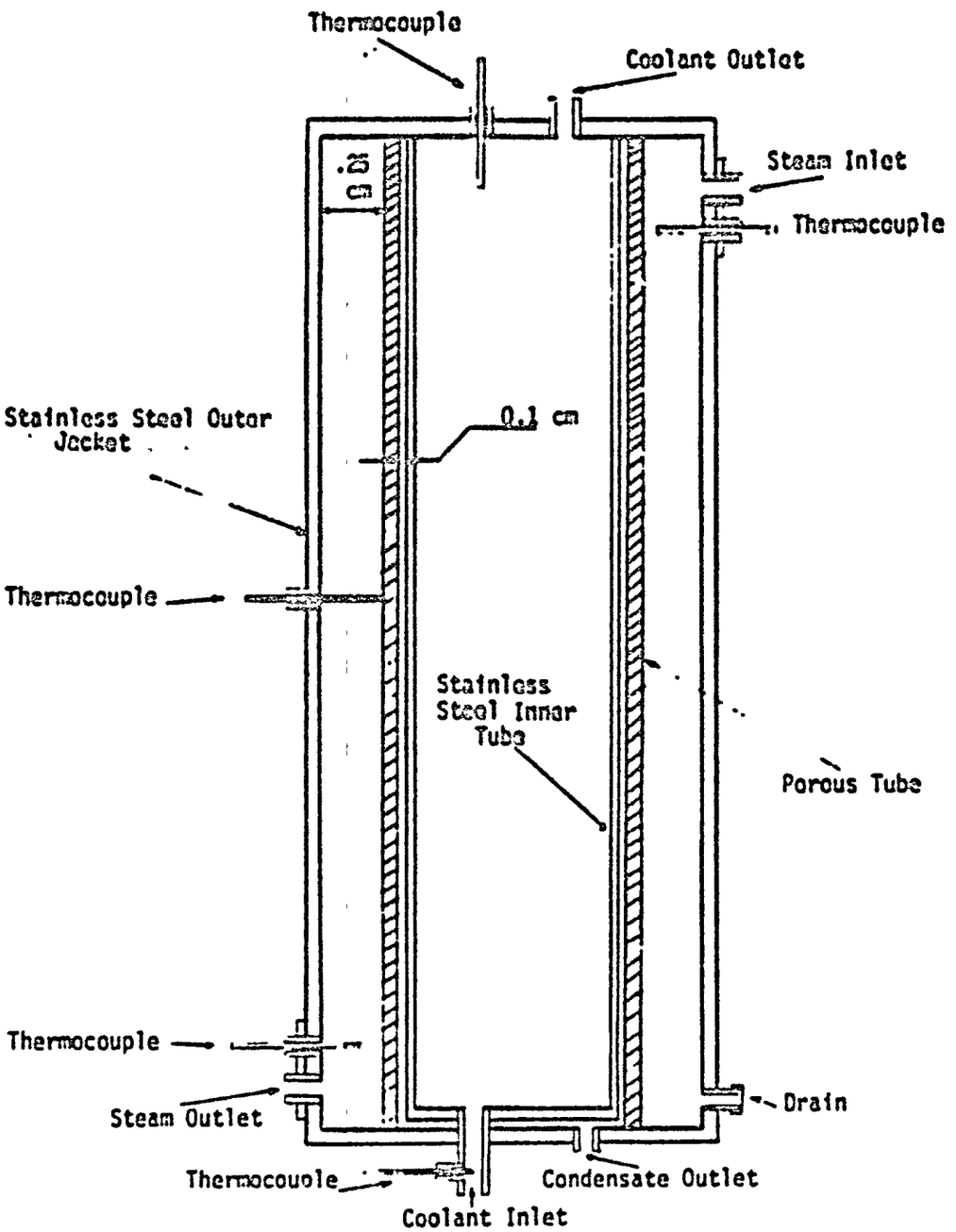

Figure 15 SCHEMATIC OF THE CYLINDRICAL CONDENSER

ORIGINAL PAGE
BLACK AND WHITE PHOTOGRAPH

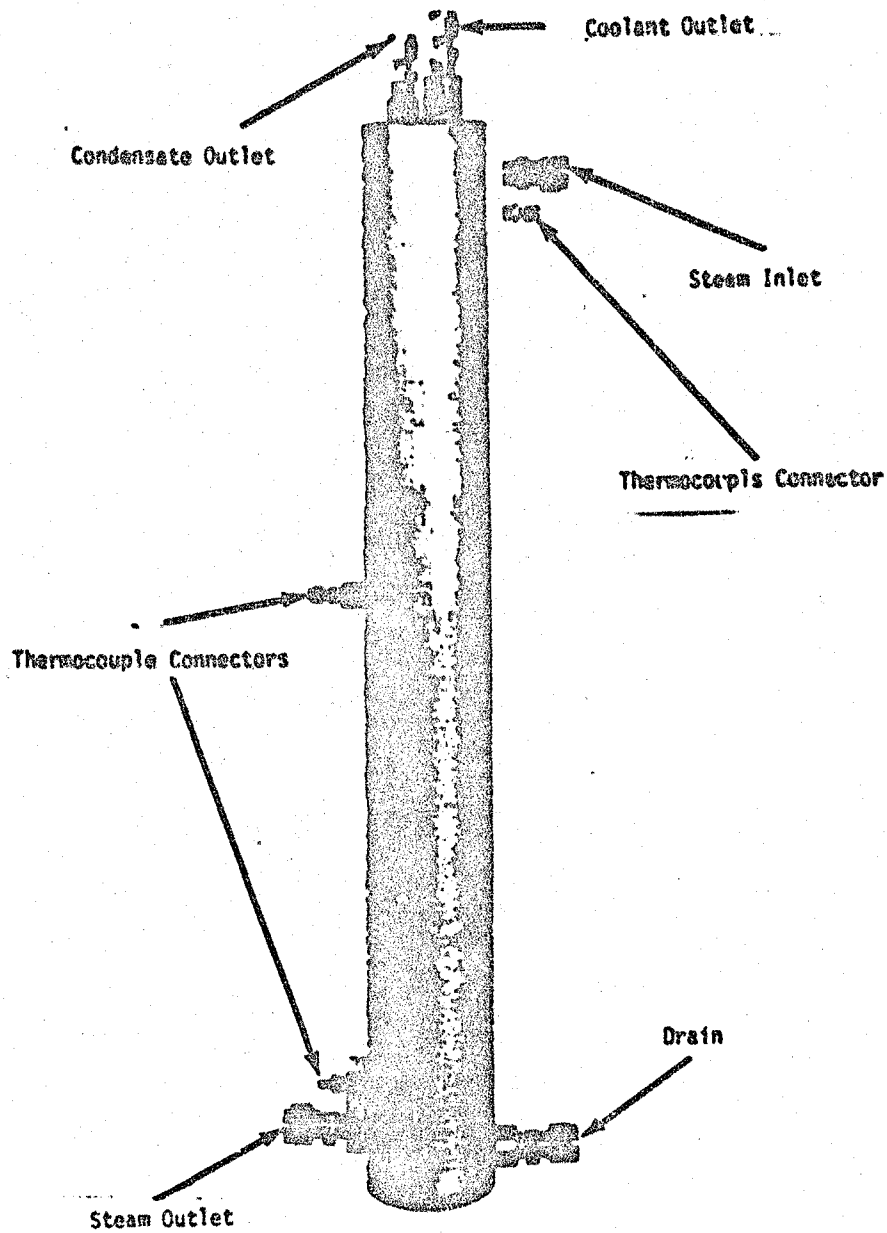

Figure 16 CYLINDRICAL CONDENSER

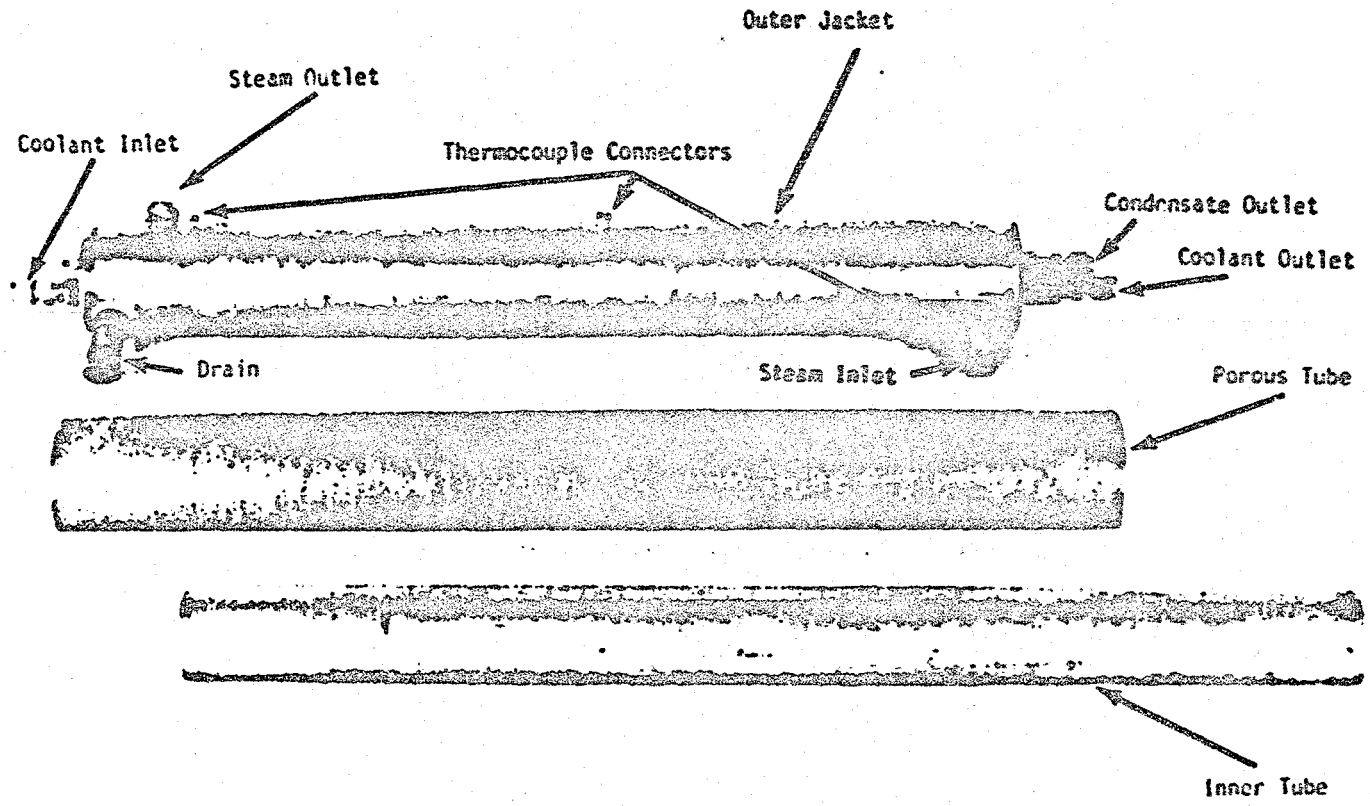

Figure 17 COMPONENTS OF THE CYLINDRICAL CONDENSER

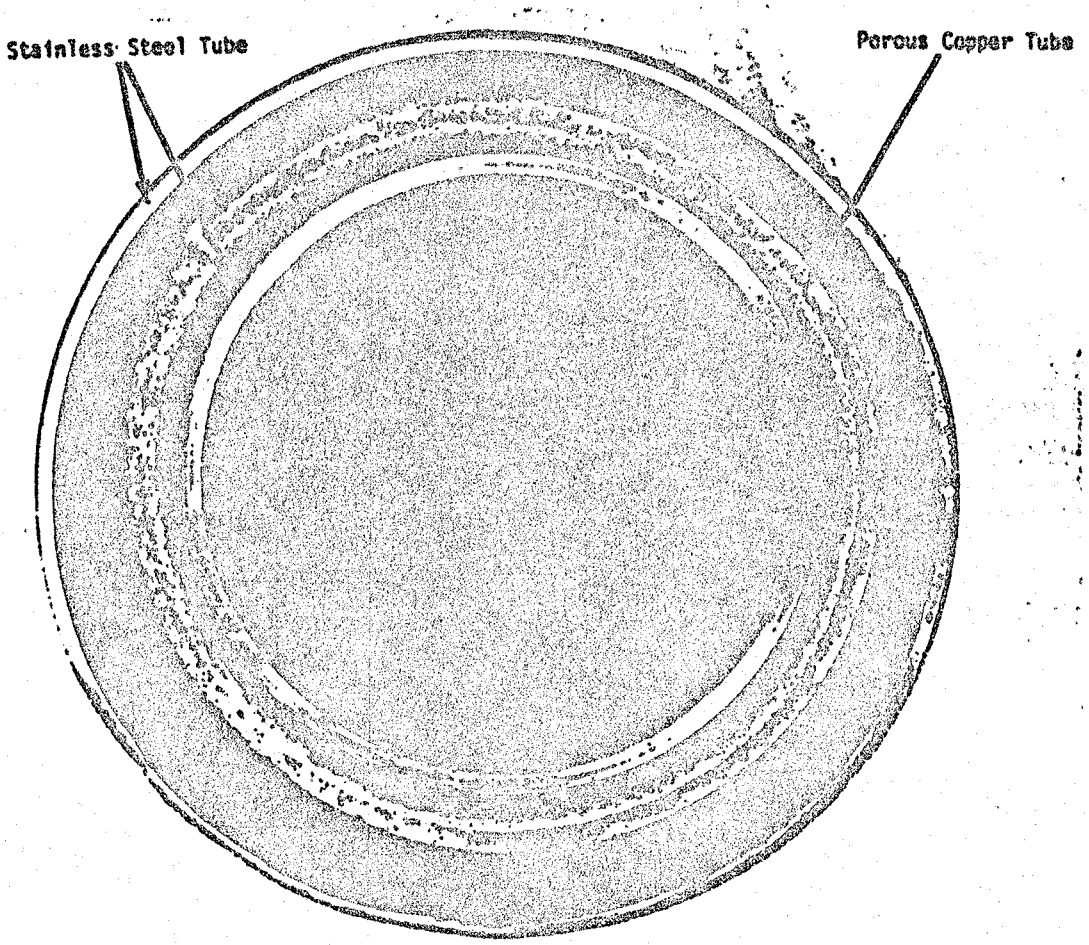

Figure 18 CYLINDRICAL CONDENSER CROSS SECTION

and flows in the annular region between the porous tube and the outer jacket. The inlet and exit ports for the coolant liquid are located at the two ends of the inner tube, and the coolant flows countercurrent to the steam flow. A gap between the inner tube and the porous tube provides the passage for collecting the recovered condensate. When steam is introduced at atmospheric pressure, the recovered condensate is removed by applying a slight vacuum to the condensate outlet; however, when steam pressure is higher than atmospheric, the condensate is pushed out automatically. Connectors are provided on the outer jacket for thermocouples and a drain. To prevent the condensation on the outer jacket, the condenser assembly is heavily insulated.

Experimental Arrangement.- The experimental set-up for testing the cylindrical condenser is shown in Figure 19. It is similar to the arrangement used with flat plate condenser; the only difference is an addition of a diaphragm-type compressor to the system. Steam is generated from distilled water in a glass boiler at a desirable rate by regulating the input voltage to the heater. Metered amounts of air are added to the vapor stream before entering the condenser. For condenser operation at pressures higher than atmospheric, the vapor-air mixture is compressed by the compressor, then delivered to the condenser. Uncondensed vapor leaving the condenser is passed through an auxiliary condenser cooled by tap water, and the volume of the condensate measured. The coolant water for the main condenser is first preheated to the desired temperature bath, then circulated countercurrently to the steam flow through the cooling side of the condenser. Inlet and outlet temperatures of steam and coolant water are measured and recorded. When the main condenser coolant temperature reaches a steady state, the test is initiated and continued for one hour.

ORIGINAL PAGE
BLACK AND WHITE PHOTOGRAPH

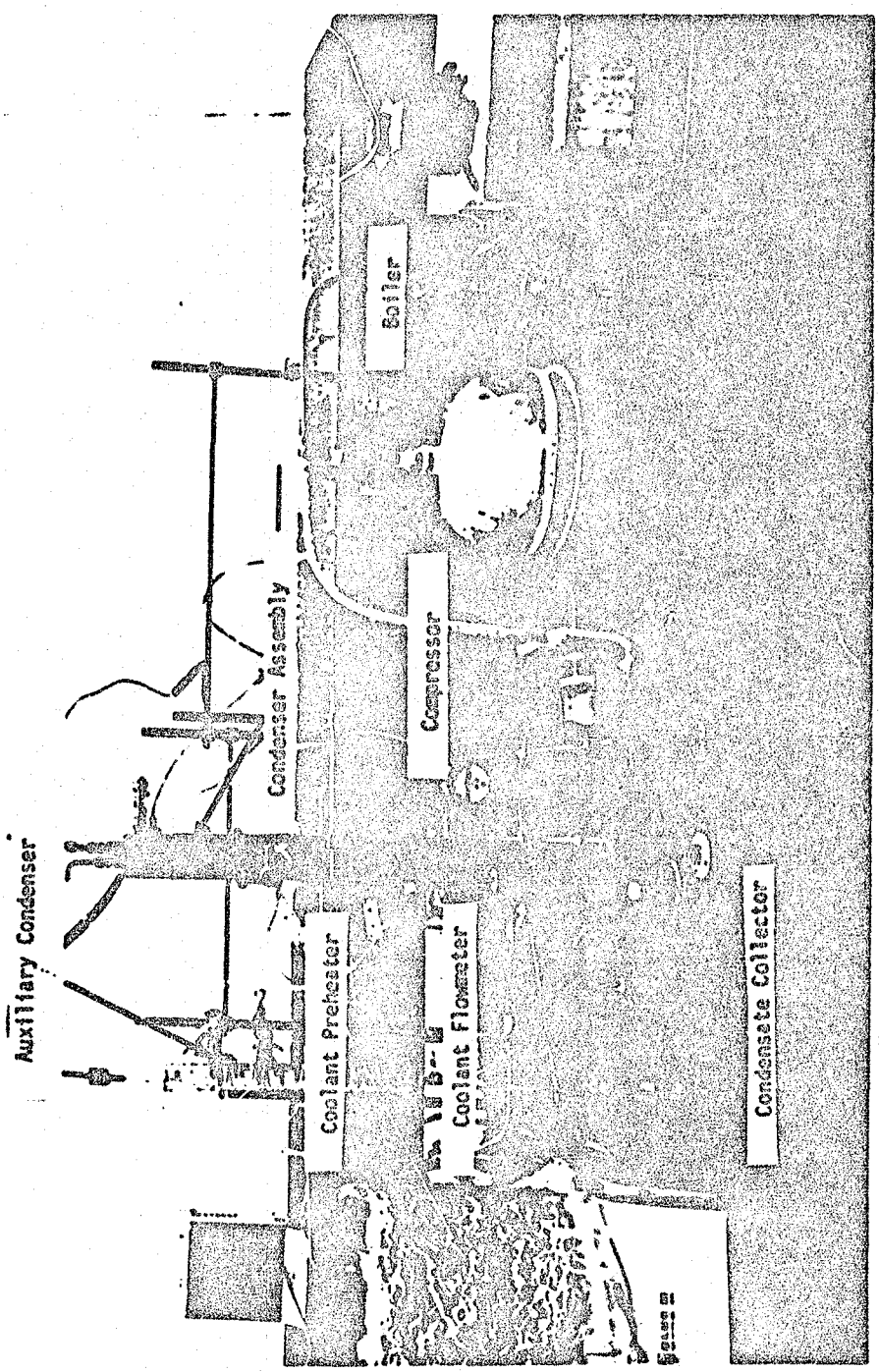

Figure 19 EXPERIMENTAL SET-UP FOR TESTING THE CYLINDRICAL CONDENSER

To determine the condenser efficiency at high pressure, the vapor/air mixture is compressed by a diaphragm-type compressor and maintained at a desired pressure level by adjusting a valve located on the condenser steam outlet; otherwise the test procedure is identical to the atmospheric pressure testing. Because the condenser pressure and the processing rates were selected as the independent variables to be maintained constant during the duration of each experiment, they determine the other independent operating parameters. Thus, the condenser pressure and flowrate determine the suction pressure of the compressor, which, in turn, affects the boiling temperature, requiring boiler heater adjustments.

Tests at Atmospheric Pressure.- The condenser was tested at atmospheric pressure using a mixture of steam and air at different coolant temperatures. The operating conditions and results for each test are presented in Table 10. The feed rates to the condenser and the condenser efficiencies under various conditions were measured in a manner discussed for flat plate condenser. As shown in Table 10, the cylindrical condenser has a high overall efficiency which is nearly independent of the coolant temperature. The theoretical rate of heat transfer to the coolant was calculated from the total heat balance across the condenser, and the actual rate was determined from the measured temperature difference and flowrate of the coolant. Except for run No. 7, which shows an unrealistic ratio of actual to theoretical rate of heat transfer, the average rate of heat transfer for other runs is about 87% of the theoretical value.

In order to check the viability of the cylindrical condenser as a zero-gravity functional unit, an experiment was performed with the condenser at a horizontal position. By placing the condenser horizontally, the

TABLE 10 OPERATION OF THE CYLINDRICAL CONDENSER AT ATMOSPHERIC PRESSURE

Run No	FEED		COOLANT			CONDENSER							
	Steam, gr/hr	Air, L/hr	Flow-Rate, ml/min	Temperature, °C		Heat Transfer Rate, KJ/hr		Temperature, °C		Recovered Water, gr/hr	Uncondensed Vapor, gr/hr		Condenser Efficiency, %
				Inlet	Outlet	Actual	Theoretical	Inlet	Outlet		Actual	Theoretical	
7	760	210	870	80.0	86.1	1295	1302	103.8	81.1	555	205	148	91
8	760	210	1050	80.0	84.4	1128	1297	102.2	80.0	550	210	137	88
9	748	210	870	73.3	79.4	1299	1526	103.8	73.3	640	108	86	97
10	771	210	870	71.1	77.2	1303	1608	103.8	71.1	672	99	74	96
11	749	210	910	68.3	74.4	1364	1599	103.3	68.3	665	84	63	97
12	760	210	870	21.1	29.5	1832	1928	103.3	21.1	740	20	4	98
13*	781	120	1650	7.2	10.5	1367	1672	107.2	10.5	620	161	1	79

* Condenser at a horizontal position.

lower half of the condenser was under a negative gravity condition. The test was performed with a mixture of 90% steam and 10% air. The condensate was collected by a suction provided at the side of the condenser. Collecting the condensate from a single side port requires relatively high vacuum, but pulling too much vacuum pulls some of the non-condensable gas to the condensate side which is undesirable. To prevent the passage of non-condensable gas, the condenser was slightly angled (15°) toward the condensate collecting side, and less than optimum vacuum was provided at the collecting port at the expense of lower efficiency. The results for this run are summarized in Table 10. The fact that the condenser is capable of performing under this condition indicates that the condenser can be a zero-gravity unit.

Tests at Pressures Higher than Atmospheric.- The experiments were performed at two condenser pressures for two different percentages of air in the mixture. The operating conditions and test results are presented in Table 11. Due to the limited capacity of the compressor, liquid process rate was about one half of the three man rate. As can be seen in Table 11, the dependent parameters such as suction pressure and boiling temperature are different for each case. After start-up, except for minor adjustments of the boiler heater to keep the suction pressure constant, the system did not require any adjustment. The condenser efficiency was calculated in a manner discussed earlier. Contrary to the expectations, the efficiency of the condenser was lower at higher pressures. The unexpected results might be due to the effect of some subcooling caused by the highly non-adiabatic behavior of the compressor.

TABLE 11 OPERATION OF THE CYLINDRICAL CONDENSER AT HIGH PRESSURE

Run No.	Feed		Compressor Suction Pressure Pa × 10^{-4}	Condenser													
	Steam, gr/hr	Air, l/hr		Inlet Temperature, °C		Outlet Temperature, °C	Pressure, Pa × 10^{-4}	Coolant			Heat Transfer Rate, kJ/hr		Recovered Water gr/hr	Uncondensed Steam, gr/hr		Condenser Efficiency,
				Measured	Calculated			Flow Rate, ml/min	Temperature, °C		Actual	Theoretical		Actual	Theoretical	
									Inlet	Outlet						
14	304	102	9.446	98.9	100.5	81.1	12.410	900	80	82.8	615	636	278	113	91	81
15	304	102	9.653	99.4	100.5	16.1	12.410	900	15.5	19.6	857	896	368	44	1	98
16	378	102	9.997	103.9	107.2	15.9	15.168	900	15.5	18.9	747	933	336	43	1	89
17	372	144	9.584	101.1	104.4	80.9	15.168	895	80	82.2	601	594	257	170	53	80
18	372	144	9.997	102.2	104.4	15.5	15.168	890	15.5	18.9	747	835	315	57	1	85

Integration of Cylindrical Condenser with the Catalyst System

The cylindrical condenser was integrated with a three-man capacity dual catalyst system to determine its efficiency under the actual operating conditions. After preliminary testing with water to determine the range of operational parameters and to establish start-up, normal running and shut-down procedures, several runs were made with untreated urine under the actual catalytic water recovery conditions.

The overall view of the system is shown in Figure 20. The main components of the system are: two catalytic reactors, the condenser, urine evaporator and gas blower. The experiment is started by preheating the catalytic reactors to their operational temperatures, followed by preheating of the urine evaporator. A measured stream of air required for maintaining the desired oxygen concentration in feed is added to the urine vapor before entering the NH_3 oxidation catalytic reactor. The vapor-air stream is passed through the NH_3 oxidation reactor, then conducted directly to the condenser. The tube connecting the catalytic reactor with the condenser is heated with a heating tape to prevent vapor condensation in the line. A gas blower, located between the condenser and the urine evaporator, recycles the non-condensable gas and the uncondensed vapor to the top of the urine evaporator. A small portion of the noncondensagle gas equivalent to the amount of added air is vented through the N_2O decomposition reactor to maintain a constant internal pressure. Tap water was used as the coolant liquid instead of feed urine because the catalytic system is not equipped with a urine recycling loop. The coolant water was preheated to the desired temperature by passing through a copper coil immersed in a

ORIGINAL PAGE
BLACK AND WHITE PHOTOGRAPH

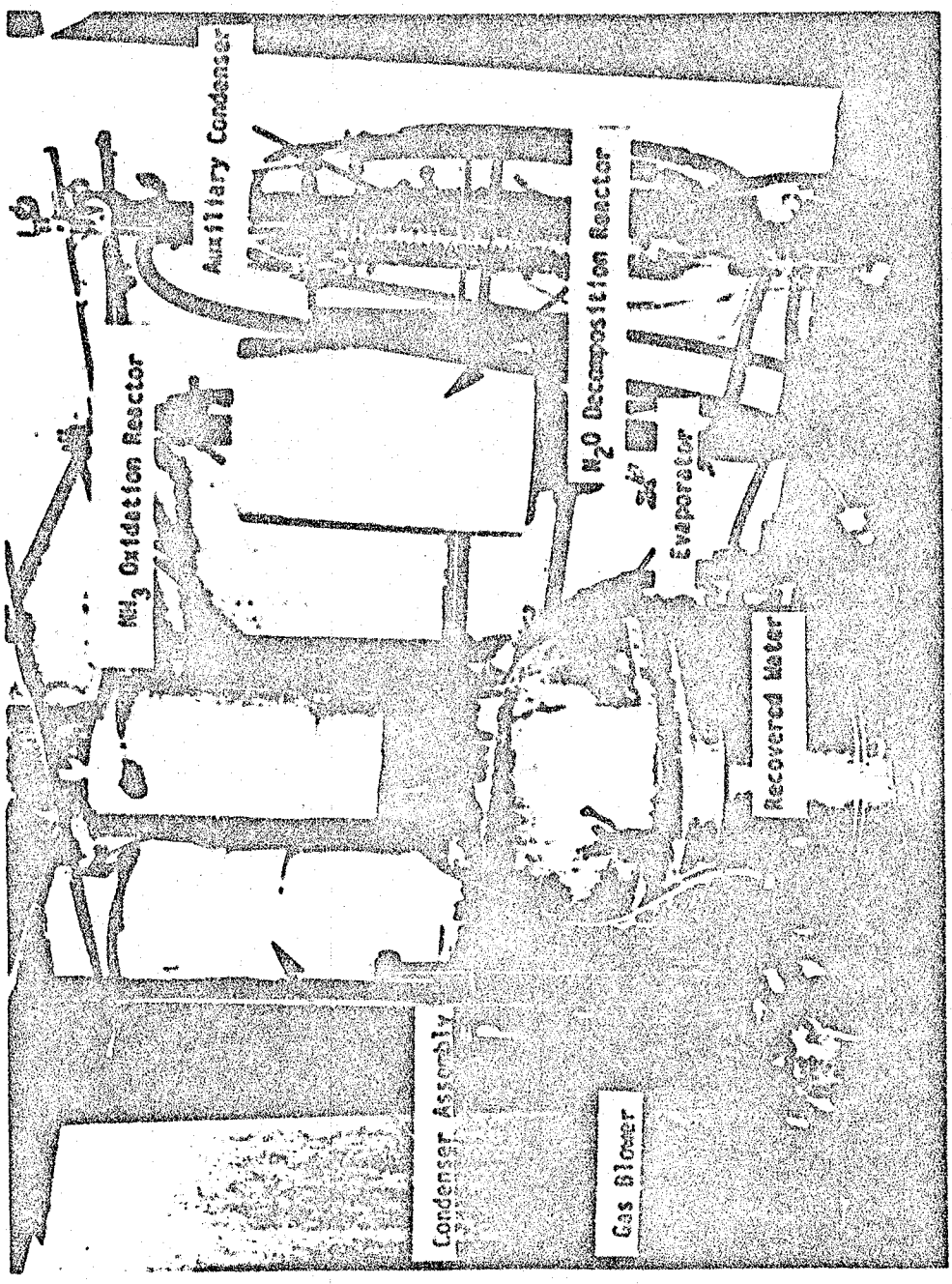

Figure 20 CYLINDRICAL CONDENSER INTEGRATED WITH DUAL CATALYST SYSTEM

constant temperature bath, then circulated through the cooling side of the condenser countercurrently to the steam.

Preliminary runs were made with water in a flow-through mode to determine the vapor generation rate under the selected conditions. The system was then converted to recycle operation and a flowmeter was temporarily placed between the gas blower and the evaporator to measure the recycle rate. After proper adjustments were made to achieve a desired recycle rate, the flowmeter was removed and the adjustments were maintained unchanged for the rest of the experiments.

All tests with urine were performed in a recycle mode using untreated urine. The liquid processing and recycling rate for these tests were assumed to be identical to the rates measured during preliminary runs with water at corresponding conditions. Each test was started after establishing a steady state condition, and was continued for one hour.

Test Results.- The experimental conditions and results for the tests with urine are summarized in Table 12. Because the vapor stream exiting the catalyst bed was fed directly to the condenser, the temperature of the vapor inlet to the condenser was higher than it would be in an efficient system employing a heat exchanger. The high vapor temperature inside of the condenser increases the heat loss through the walls and, thus, decreases the ratio of the observed to theoretical heat transfer rates. For an efficient operation, the vapor should be cooled close to the saturation temperature before entering the condenser.

The average condenser efficiency for collecting wastes was approximately 90% and decreased with the increase in coolant temperature, as expected. These tests indicate that the condenser is capable of performing

TABLE 12 OPERATION OF THE CONDENSER INTEGRATED WITH THE CATALYTIC SYSTEM

Vapor Feed: 612 gr/hr
Air Feed: 43.5 L/hr
Recycle Rate: 240 L/hr

Run No	Catalyst Bed Temperature, °C	CONDENSER										
		Temperature, °C		Coolant			Heat Transfer Rate, KJ/hr		Recovered Water, ml/hr	Uncondensed Vapor, ml/hr		Condenser efficiency, %
		Inlet	Outlet	Flow Rate, ml/min	Temperature, °C		Actual	Theoretical		Actual	Theoretical	
					Inlet	Outlet						
19	293.3	184.4	10.0	1100	5.6	9.4	1048	1611	573	39	2	94
20	279.4	181.1	61.7	1045	60.0	63.3	665	1294	498	114	58	90
21	283.3	191.1	73.9	1060	71.1	73.9	738	1084	426	186	123	87

satisfactorily at high coolant temperatures required if direct heat transfer to urine recycle loop is employed.

CONCLUSIONS AND RECOMMENDATIONS

Based on the analytical evaluation of conceptual evaporation/condensation systems and test data obtained during this investigation, the following conclusions can be made:

1. An energy efficient evaporation/condensation concept suitable for integration with the catalytic water recovery system combining the energy efficiency of the VCD with the mechanical simplicity of TIMES was identified.
2. A cylindrical condenser suitable for a three-man rate catalytic water recovery system and capable of condensing water vapor in the presence of up to 20% noncondensable gases at atmospheric or elevated pressures was developed.
3. The cylindrical condenser has an average condensation effiency of approximately 90% at various coolant temperatures.
4. The condenser recovers and transfers the heat of condensation to the coolant, which in the actual system will be the feed urine The average rate of heat transfer to the heat sink is about 85% of the theoretical value.
5. The condenser functions equally well in any position; therefore, it can be assumed that it is suitable for zero-g conditions.
6. The condenser performed satisfactorily integrated with the dual catalyst system under the actual operating conditions with untreated urine. The observed average condensation efficiency of the condenser with the dual catalyst system was about 90%.

To make the catalytic water recovery system viable for spacecraft applications, the development of evaporation/condensation concept found suitable for integration with the catalytic method is recommended. Since many components have been previously tested in similar applications and the condenser for condensing recovered water with transfer of energy to feed urine in the presence of noncondensables has been developed during this program, there should be no unsurmountable problems for the development of an integrated system.

REFERENCES

1. Rohsenow, W.M., "A Method of Correlating Heat Transfer Data for Surface Boiling of Liquids," Trans. ASME, 74, pp. 969-975 (1952).
2. Putnam, D.F., "Composition and Concentrative Properties of Human Urine," DAC-61125-F1, June 1970.
3. Rohsenow, W.M. and Hartnett, J.P., "Handbook of Heat Transfer."
4. Gertsmann, J. and Griffith, P. "Effect of Surface Instability on Laminar Film Condensation," Int. J. Heat Mass Transfer, 10,567 (1967).
5. Sparrow, E.M. & Minkowycz, W.J., "Condensation Heat Transfer in the Presence of Non-Condensables, Interfacial Resistance, Superheating, Variable Properties and Diffusion," Int. J. Heat and Mass Transfer 9, pp. 1125-1144 (1966).
6. Collier, J.G., "Convective Boiling and Condesnation," McGraw-Hill, (1972).
7. Kroger, D.G., "M.I.T. Heat Transfer Lab Report 75239-42," Sept. 1966.
8. Trusch, R.B., and Roebelen, G.J. Jr., "A Thermoelectric Integrated Membrane Evaporation System," ASME Publications 78-ENAs-19.
9. Brouillet, A.O., and Boynton, C.K. Jr. "Applications of the Thermo-electrically Integrated Membrane Evaporator Subsystem," ASME Pub. 79-ENAs-48.
10. Winkler, H.E. and Roebelen, G.J. Jr., "Development of a Preprototype Thermoelectric Integrated Membrane Evaporation Subsystem for Water Recovery," ASME Pub. 80-ENAs-46.
11. Bird, R.B., Stewart, W.E. and Ligthfoot, E.N., "Transport Phenomena" John Wiley & Sons, 1960.

12. Thompson, C.D., Ellis, G.S., Schubert, F.H., "Preprototype Vapor Compression Distillation Subsystem Development," ASME Pub. 81-ENAs-25.

13. Kern, Q.D., "Process Heat Transfer," McGraw-Hill, 1978.

1. Report No.	2. Government Accession No.	3. Recipient's Catalog No.
NASA CR-166478		

4. Title and Subtitle	5. Report Date
Development of a Condenser for the Dual Catalyst Water Recovery System	March 1983
	6. Performing Organization Code
7. Author(s)	8. Performing Organization Report No.
P. Budininkas, F. Rasouli, and N. Rabadi	199-60-12-10
	10. Work Unit No. T-4589
9. Performing Organization Name and Address	11. Contract or Grant No.
GATX/GARD, Inc. 7449 North Natchez Avenue Niles, Illinois 60648	NAS2-11045
	13. Type of Report and Period Covered
12. Sponsoring Agency Name and Address	Contractor Report
National Aeronautics and Space Administration Washington, D.C. 20546	14. Sponsoring Agency Code

15. Supplementary Notes

Point of Contact: Tech. Monitor: P.D. Quattrone, MS:239-4, Ames Research Center, Moffett Field, CA 94035
415-965-5733 or FTS-448-5733

16. Abstract

The recovery of potable water from untreated urine by the catalytic method has been previously demonstrated; however, to minimize the energy requirements, the catalytic system must be integrated with an energy efficient, zero-gravity evaporative process.

The first phase of this program consisted of a study and analytical evaluation of conceptual evaporation/condensation systems suitable for integration with the catalytic water recovery method. The primary requirements for each concept were its capability to operate under zero-gravity conditions, condense recovered water from a vapor-noncondensable gas mixture, and integrate with the catalytic system. Specific energy requirements were estimated for concepts meeting the primary requirements, and the concept most suitable for integration with the catalytic system was proposed.

A Three-man rate condenser capable of integration with the proposed system, condensing water vapor in presence of noncondensables and transferring the heat of condensation to feed urine was designed, fabricated, and tested. It was tested with steam/air mixtures at atmospheric and elevated pressures and integrated with an actual catalytic water recovery system. The condenser has a condensation efficiency exceeding 90% and heat transfer rate of approximately 85% of theoretical value at coolant temperatures ranging from 7°C to 80°C.

17. Key Words (Suggested by Author(s))	18. Distribution Statement
Catalyst Water Recovery Condenser	UNCLASSIFIED-UNLIMITED STAR Category - 54

19. Security Classif. (of this report)	20. Security Classif. (of this page)	21. No. of Pages	22. Price*
UNCLASSIFIED	UNCLASSIFIED	80	

*For sale by the National Technical Information Service, Springfield, Virginia 22161

End of Document